Metal-substituted microporous aluminophosphates

Gopinathan Sankar[1] and Manuel Sánchez-Sánchez[2]

[1]Department of Chemistry, University College London, 20 Gordon Street, London WC1H 0AJ, UK. E-mail: g.sankar@ucl.ac.uk

[2]Instituto de Catálisis y Petroleoquímica (ICP), CSIC, C/ Marie Curie, 2. 28049 Madrid, Spain. E-mail: manuel.sanchez@icp.csic.es

Abstract

This Chapter aims to present the zeotypes aluminophosphates (AlPOs) as a complementary alternative to zeolites in the isomorphic incorporation of metal ions within all-inorganic microporous frameworks as well as to discuss didactically the catalytic consequences derived from the distinctive features of both frameworks. It does not intend to be a compilation of either all or the most significant publications involving metal-substituted microporous aluminophosphates. Family of AlPOs and zeolites, which includes metal ions substituted variants, are the dominant microporous materials. Both these systems are widely used as catalysts, in particular through aliovalent metal ions substitution. Here, some general description of the synthesis procedures and characterization techniques of the MeAPOs (metal-contained aluminophosphates) is given along with catalytic properties. Next, some illustrative examples of the catalytic possibilities of MeAPOs as catalysts in the transformation of the organic molecules are given. The oxidation of the hardly-activated hydrocarbons has probably been the most successful use of AlPOs doped with the divalent transition metal ions Co^{2+}, Mn^{2+} and Fe^{2+}, whose incorporation in zeolites is disfavoured. The catalytic role of these MeAPOs is rationalized based on the knowledge acquired from a combination of the most advanced characterization techniques. Finally, the importance of the high specificity of the structure-directing agents employed in the preparation of MeAPOs is discussed taking N,N-methyldicyclohexyamine in the synthesis of AFI-structured materials as a driving force. It is shown how such a high specificity could be predicted and how it can open great possibilities in the control of parameters as critical in catalysis as crystal size, inter- and intracrystalline mesoporosity, acidity, redox properties, incorporation of a great variety of heteroatom ions or final environment of the metal site (surrounding it by either P or Al).

1. Microporous crystalline AlPOs

Since the discovery of natural zeolites [1], more than two and a half centuries ago, these materials were considered as crystalline aluminium-containing tectosilicates having pores of molecular dimension. The definition continues to exist, even today, with more than 230 different zeolite structures have been identified [2,3]. Any of the three mentioned key properties of zeolites, i.e. crystallinity, molecular-size porosity (microporosity) and aluminosilicate composition, has been extensively studied and exceeded. In this context, it is particularly highlighted the alteration in composition, primarily due to the incorporation of numerous heteroatom ions, others than Si^{4+} and/or Al^{3+}, into the zeolitic frameworks. As a consequence of such heteroatom incorporation, Ti-zeolites [4], B-zeolites [5], V-zeolites [6], Zr-zeolites [7], Sn-zeolites [8], Fe-zeolites [9, 10], Ga-zeolites [10], Ge-zeolites [11] and other heteroatom-zeolites [12-14], have been investigated widely. All of them have SiO_4 tetrahedra as the basic and more abundant unit, they do not necessarily contain Al and the heteroatom ions are part of the zeolite framework occupying tetrahedral sites. The incorporation of these metallic heteroatoms within the zeolitic framework is not limited to an academic exercise but allows these materials to reach new industrial catalytic applications [12]. In this sense, in previous Chapters of this issue, countless examples of applications of metal-zeolites, particularly focused on the field heterogeneous catalysis, which are unable to be reached by their counterpart metal-free zeolites, have been presented.

In metal-zeolites, the metal is almost always a dopant in terms of its loadings against that of the predominant Si. Al^{3+} is the only heteroatom ion able to be quantitatively closer to Si in certain zeolites, including in the natural ones. However, there are other inorganic oxide-based materials, which are also crystalline and possess microporosity but they are not based on SiO_2 [15, 16]. In addition, some of these materials are closely related to zeolites in critical properties as their microporous crystalline structures or their thermal/hydrothermal stability. All these similarities led to name these materials as zeotypes, denoting the various likenesses with the zeolites family and, at the same time, highlighting that they are not zeolites. Nevertheless, it is quite common to even refer them as zeolites [17-19].

Therefore, zeotypes can be defined as materials that have crystalline and microporous frameworks having similar physical and chemical properties of aluminosilicate zeolites, but whose atoms at the tetrahedral sites are not silicon or aluminium, e.g. cobalt phosphate [20] zincophosphate [21], beryllophosphate [21] aluminophosphates [22, 23], nickel phosphates [24], gallium phosphates [25] or beryllium hydroxides [26], among many others. Microporous frameworks based on metal-phosphates are particular abundant [27]. Among these zeotypes, the microporous aluminophosphates, also known as AlPOs ($AlPO_4$ or simply AlPO in singular) have been the most investigated for so many reasons. Firstly, they were the first described zeotypes [22, 23], and indeed the term zeotype was introduced to integrate $AlPO_4$ materials within the ‘zeolite World’. Besides, they have thermal stability quite similar to that found in zeolites and much higher than most of other zeotypes. Like pure SiO_2 zeolites, in the absence of heteroatom ions, they are neutral and isoelectronic with zeolites since the sum of the formal charges of an Al^{3+} ion and a P^{5+} ion, which are strictly alternated in an $AlPO_4$ framework, equal to the charge of two contiguous Si^{4+} ions in a zeolite. Moreover, many of the $AlPO_4$-based materials have common topologies with zeolites [2, 3]. Finally, and maybe the most important reason, AlPOs have contributed the family of microporous materials that expand the structures and the (catalytic) applications of zeolites. The following three cases are excellent examples: (i) until the relatively recent discovery of ITQ-33 [28] and ITQ-37 [29], the $AlPO_4$ material known as VPI-5 [30] (IZA three-letter code VFI [2, 3]) allowed zeolitic family to ‘boast’ of pore entrances as large as 12 Å through an 18-R pore (rings having 18 tetrahedral atoms plus 18 oxygens); (ii) the implantation of several industrial plants to produce olefins from methanol in the very recent years in China [31, 32], is a first but important starting point to reduce the undesired energetic and chemical dependency of petroleum; such process is catalysed by the Si-doped small pore $AlPO_4$-34, the so-called SAPO-34; (iii) the possibility of directly incorporation divalent transition metal ions in the Al positions of a $AlPO_4$ material, which is not obvious in zeolites because it implies a charge balance problem, led to materials such as CoAPOs, MnAPOs, ZnAPOs, etc. [33, 34], some of which resulted active as catalysts in the direct oxidation of the low-reactive hydrocarbons with oxygen [35-37]. Precisely the latter is closely related to both the scope and the focus of this issue in general and this present Chapter in particular.

Apart from these selected examples, AlPOs as zeotypes can contribute with singular features, hardly found in zeolites. Table 1 summarizes some of these singularities of AlPOs compared to the corresponding properties of conventional zeolites, thinking in terms of their ability to incorporate heteroatoms and their catalytic applications.

Table 1. Comparison of some properties between conventional zeolites and $AlPO_4$ zeotypes.

Property	Zeolites	AlPOs
Hydrophilic/hydrophobic character	Hydrophobic (tuned to hydrophilic co-incorporating Al)	Hydrophilic
pH of the synthesis gel	Basic	Acidic-neutral
Predominant SDA nature	Quaternary Ammonium	Amines
Phase-specificity of SDAs	Medium	Low
Incorporable oxidation state	3+ and 4+	2+ to 5+
Framework charge	No (if Al-free)	No
Known topologies	200+	ca. 50
Proportion of 1D topologies[a]	25 %	40 %

[a]Percentage of 1D topologies with respect the whole known structures. In the case of AlPOs, only the structures able to be prepared as a non-doped $AlPO_4$ form have been considered.

In spite of the significant similarities between AlPOs and zeolites, Table 1 makes clear that both families of microporous materials have very different behaviour in various aspects either directly or indirectly related to the incorporation of transition metal ions within their frameworks. Next, the different properties compiled in Table 1 will be developed more extensively.

1.1. Hydrophilicity/hydrophobicity

Hydrophilicity/hydrophobicity of solid materials is a key parameter in several industrial applications, but becomes even more important if the material is used taking advantage of their porosity. A way to measure this parameter is through water adsorption isotherms (Figure 1A [38]). $AlPO_4$ frameworks, which provide water isotherms either type I with sorption equilibrium at relatively high relative pressure or type V (Figure 1B [39]), are much more hydrophilic than SiO_2 frameworks (type VII isotherms). However, the Al-rich zeolites give isotherms type I with equilibrium reached at low pressures, and are much more hydrophilic than AlPOs (Figure 1B [39]). This is because SiO_2 framework are neutral whereas the notable hydrophilicity of low Si/Al ratio zeolites is due to their negatively charged framework and to the presence of charge compensating extra-framework cations, whose nature is controllable by its ion exchange capacity [38]. The huge hydrophilicity/hydrophobicity range given by zeolites allows them to find applications in fields as diverse as water adsorption (the hydrophilic zeolites) or certain catalytic oxidation of organic molecules in liquid phase (generally requiring hydrophobic zeolites). The medium hydrophilicity of AlPOs [38], which is difficult to be tuned, becomes a drawback when compared to zeolites in any of these applications.

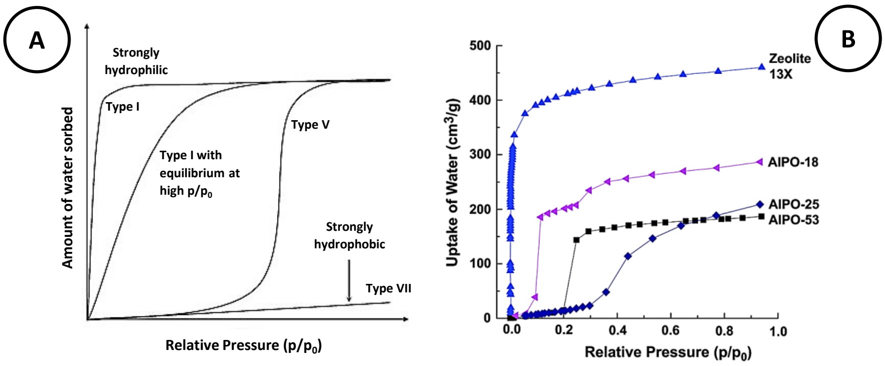

Figure 1. A) Models of water sorption isotherms of four nanoporous solids with different degrees of hydrophilicity. Adapted from Microporous Mesoporous Mater, 114, E. P. Ng et al., Nanoporous materials with enhanced hydrophilicity and high water sorption capacity, 1-26, Copyright 2007, with permission from Elsevier [38]. B) Experimental water adsorption isotherms of various narrow pore AlPOs at 293 K, compared with the zeolite 13X. Reproduced from ref. [39] with permission of The Royal Society of Chemistry.

Nevertheless, as mentioned previously in this Chapter, AlPOs can be doped by certain heteroatom ions, mainly divalent or tetravalent ones, whose introduction into the framework makes these materials negatively charged. Like Al-containing zeolites, these charged AlPOs can be potentially ion exchanged to enhance their hydrophilic character [40]. However, this strategy is far from reaching the hydrophilic character of zeolites due to two important limitations. It is difficult to incorporate high loadings of heteroatoms in AlPOs similar to Al in zeolites, which could reach Si/Al as low as 1; Si is the heteroatom that can be incorporated at highest concentration in AlPOs but when concentrated, it tends to form SiO_2 islands where only part of the incorporated Si introduces charge in the $AlPO_4$ framework. Indeed, the amount of isolated Si incorporated is theoretically limited to around 12.5 % of the tetrahedral (P) sites [41, 42], far from the 50 % of Al found in zeolites with a Si/Al ratio of 1. Microporous Co-rich aluminophosphates have also been reported [43]. These materials are cobalt phosphates doped with Al but, to the best of our knowledge, they are not stable when the organic structure directing agent is removed and loose its porosity because of their low stability to calcination. As a consequence, the ion exchange in AlPOs has been less investigated and could hardly provide any real contribution to the hydrophilic-related applications of Al-zeolites.

In any case, making the AlPOs hydrophobic, which would be them closer to zeolites for certain catalytic applications of interest in this Chapter, is intrinsically avoided by their own aluminophosphate nature. On the contrary, the already-hydrophobic Al-free zeolites can become even more hydrophobic by changing the conventional synthesis mineralizing agent OH- by a fluoride medium, which allows the preparation of zeolites free of hydrophilic Si-OH defects [44, 45].

1.2. pH of the synthesis

pH value of the starting gels is undoubtedly one of the most determinant parameters in controlling the kinetics of the zeolite crystallization, but also in terms of the nature of the crystallized phase(s), the amount of defects, the Si/Al ratio, etc. [46]. The synthesis of conventional zeolites, which are prepared in OH^- media, is carried out at very alkaline pH, commonly covering the pH range of 10-13. As an alternative to OH^- as the mineralizing agent, F^- can be also used for the preparation of zeolites at lower pHs, between 7 and 12, which result in practically a defect-free form [45].

The synthesis of AlPOs can be carried out starting from gels of pH values in the range 3-10, although the most common pHs are acid, between 3 and 7. From gels with pH below 3, normally dense (i.e. non-porous) phases such as tridymite, cristobalite or $AlPO_4$ hydrated are formed [47]. Thinking in terms of incorporation of metal ions within these two microporous frameworks, it is convenient to be aware of the existence of the different thermodynamically-stable metal species in aqueous solution along the all pH range. Figure 2 shows the Pourbaix diagram of cobalt as an example. Pourbaix diagrams maps out the possible stable (equilibrium) phases of a metal as a function of pH and electrochemical potential of the solution [48]. In aqueous solution, the stable species are these included between the oblique dashed dotted lines denoted as ‘a’ and ‘b’, which delimits the oxidation and reduction voltage potentials of water. Like most transition metal, cobalt is soluble at low pH. In particular, cobalt is stable as soluble Co^{2+} in the pH range from -2 to around 9. Above pH 9, Co is found in a solid form, either as Co(OH)$_3$ or mainly as Co(OH)$_2$. It implies that, in aqueous solution and in the absence of any other chemical species, the most stable Co species (and in general any transition metal species) are different at the typical pH of the synthesis of zeolites (9-13) and at that of the synthesis of AlPOs (3-7). It is presumably that this fact has a strong influence on the way in which transition metal ions are incorporated in zeolites or in the zeotypes AlPOs, beyond the environmental and/or crystallographic restriction intrinsically imposed by each framework. In our opinion, this aspect has not been addressed with enough clarity in the literature yet.

Commented [ms1]: **Joaquín commented:** But according to the diagram, Co soluble species are not stable at pH > 9, and this indeed make a difference with AlPO. Please revise this sentence.
Answer: That is exactly what we meant, that the most stable Co species are different under the conditions at which AlPOs and zeolites are prepared. We modify the sentence trying to clarify this fact.

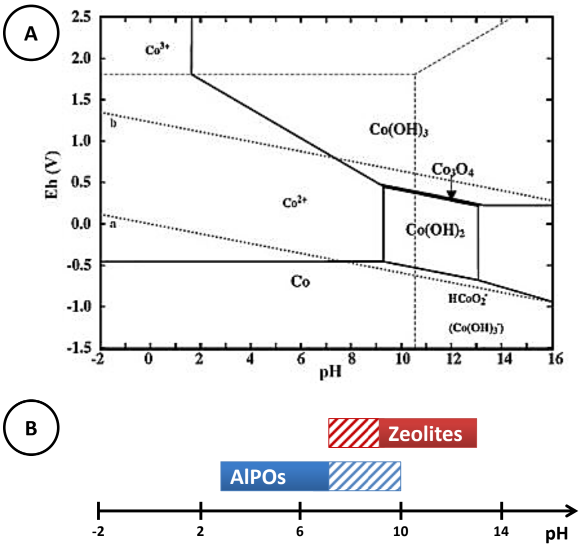

Figure 2. (A) Pourbaix diagram of cobalt. The thermodynamically-stable species in aqueous solution are these found between the segment delimiting by dotted lines *a* and *b*. (B) Scheme of the pH range at which zeolites (red region) and AlPOs (blue region) are normally prepared. The stripped region represents pHs at which AlPOs (blue) and zeolites (red) can also be prepared beyond conventional pHs.

1.3. Nature and phase-specificity of structure-directing agents

Generally speaking, the most conventional structure directing agents of the zeolites are alkaline hydroxides for low Si/Al zeolites and quaternary ammonium hydroxides for high Si/Al zeolites [49, 50], whereas amines are the most preferred structure-directing agents (SDAs) for AlPOs [51]. That observation finds so many exceptions in the literature. The most evident one is that AlPOs can be prepared with quaternary ammonium hydroxides [52, 53] and zeolites can be prepared with certain amines [54, 55]. The reason behind the extensive use of either inorganic or organic hydroxides in the synthesis of zeolites and the less basic amines for the synthesis of AlPOs, is evidently related to the required pH by the silica- or aluminophosphate-based materials to be crystallized (Figure 2).

Table 2 compiles the nature of the SDAs most frequently used in the preparation of different AlPOs/MeAPOs. The prevalence of amines as SDA of AlPOs is marked form Table 2. On the other hand, the large number of organic molecules able to direct the crystallization of certain AlPOs, particularly these having AFI and AEL topologies, indicates that in general amines has low phase specificity. As an example, 23 different organic SDA were reported to direct the crystallization of $AlPO_4$-5 in 1983 [56], just one year after $AlPO_4$ materials were patented [22]. Similarly, some amines like DPA are able to direct the crystallization of several $AlPO_4$-based materials with different topology [57-59]. The specificity of organic SDA in zeolites is normally much higher, in spite of their role was reduced from the ambitious concept of 'template' to the simple SDAs some decades ago [49]. The importance of the specificity and the efficiency of a given SDA towards a particular topology is made clear in a below section of this Chapter expressly dedicated to that subject (Section 5).

Commented [ms2]: Joaquín commented: This should be most probably ref 49.
Answer: It is indeed ref. 49. Thanks.

Table 2. $AlPO_4$ materials accepted by IZA and their homologues doped with heteroatom ions. The dimensionality of their pore system, the number of tetrahedral atoms in their largest ring, their common names and the structure-directing agents are also given. Si has been discarded as heteroatom ion as it is out of the scope of this Chapter.

nD[a]	MR[b]	IZA code[c]	$AlPO_4$-n[d]	Incorporated Me[e]	SDA[f]
1D	18R	VFI	VPI-5/$AlPO_4$-54	None, Co, Mg, Mn, Ti, Fe, Cr, V	None, DPA, TBAOH
	14R	AET	$AlPO_4$-8	None, Mn	By heating VPI-5
	12R	AFI	$AlPO_4$-5	None, Co, Zn, Mg, Mn, Ti, Fe, Cr, Ni, V, Cu, Mo, Sn, Zr, Ca, Sr, Ba, Be, Ge, Li, Ce, Cd, Ru	TEA, TEAOH, TPA, TPAOH, MCHA and 50+ more amines
		ATO	$AlPO_4$-31	None, Co, Zn, Mg, Mn, Ti, Cr, V, Cu, Cd	DPA, DBA, DPentA, DHA, HMI
		ATS	$AlPO_4$-36	None, Co, Zn, Mg, Mn, Ti, Fe, V, Be, Ga	TPA, ECHA, DPBA
		SAF	STA-15	None	TPAOH
		AEL	$AlPO_4$-11	None, Co, Zn, Mg, Mn, Ti, Fe, Cr, Ni, V, Cu, Nb, As, Be, Ge, Cd	DPA, DiPA, DiBA and a few more

	10R	AFO	$AlPO_4$-41	None, Co, Mn, Ti, V, Zr	DPA, DiPA, DiPFA, DEA, DBA, DPentA,
		JRY	CoAPO-CJ40	Co, Zn, Mn, Fe	DEA
		AHT	$AlPO_4$-H2	None	None
	8R	ATN	$AlPO_4$-39	None, Co, Zn, Mg	DPA, DiBA
		ATV	$AlPO_4$-25	None, Co	By heating $AlPO_4$-21
		AWW	$AlPO_4$-22	None	HMTA, HMI, MDEA, DDO
2D	12R	AFR*	$AlPO_4$-40	None, Co, Zn	TPAOH (+ TMAOH)
		SBE*	UCSB-8Co	Co, Zn, Mg, Mn	DAN
		SFO*	SSZ-51	None, Co	DMAP
	8R	AEN	$AlPO_4$-EN3/-53	None, Co, Mn, Cu	MA, DMA
		AFV	$AlPO_4$-57	Zn, Mg	DEDMA
		APC	$AlPO_4$-C	None, Co	By heating $AlPO_4$-H3
		APD	$AlPO_4$-D	None	By heating $AlPO_4$-C
		ATT	$AlPO_4$-33	None	TMAOH
		AVL	$AlPO_4$-59	Zn, Mg	ETMA
		AWO	$AlPO_4$-21	None	EA, pirrolidine, TEA, PA, MDEA, etc.
		LEV	$AlPO_4$-35/-67	None, Co, Zn, Mg	HEM, TrOH, DABCO, ETMA, DEDMA, MCA
		OWE	ACP-2/UiO-28	Co, Mg	DET
		ZON	ZnAPO-M1	None, Co, Zn, Mg	TMAOH
3D	12R	AFS*	$AlPO_4$-46	Co, Zn, Mg, Mn, Ni	DPA
		AFY*	$AlPO_4$-50	Co, Zn, Mg, Mn	DPA
		DFO*	DAF-1	Co, Mg, Ni	DMOH
		FAU	$AlPO_4$-37	Co, Zn	TPAOH + TMAOH
		SAO	STA-1	Zn, Mg	BPM, BP
		SBS	UCSB-6	Co, Zn, Mg, Mn	DAH
		SBT	UCSB-10	Co, Zn, Mg	TTD
	8R	AEI	$AlPO_4$-18	None, Co, Zn, Mg, Mn, Ti, Fe, Ni, V, As, Ge, Ga	TEA, TEAOH, DiPE
		AFN	$AlPO_4$-14	None, Co, Zn, Mg, Mn, Cr,	PDA, DABCO, iPA, tBA
		AFT	$AlPO_4$-52	None	TEAOH + DPA
		AFX	$AlPO_4$-56	Co, Mn, Zr	TMHD
		ANA	$AlPO_{4-}$24	None, Co	Na+, Cs+
		CHA	$AlPO_4$-34	None, Co, Zn, Mg, Mn, Fe, Cr Ni, Cu, Be, Li	TEAOH, TEA, DPA, DEA, MA and others
		DFT	DAF-2	Co	EDA
		EDI	Edingtonite	Co	1,2-DAP
		ERI	$AlPO_4$-17	None, Co, Mg, Fe	Q, NPA, CA, piperidine
		GIS	$AlPO_4$-43	None, Co, Zn, Mg	DPA
		LTA	$AlPO_4$-42	None, Co, Zn, Mg, Mn, Fe	TMAOH + Na+
		MER	Merlinoite	Co	DMA
		PHI	DAF-8	Co, Zn	DACH
		RHO	Rho	Co, Mg, Mn	DiPPD

	SAT	STA-2	Mg	BQNB
	SAV	Mg-STA-7	Co, Zn, Mg	tmtact, hmhaco
	SIV	SIZ-7	Co	EMIm
	THO	Thomsonite	Co	MEDA

[a] Dimension of the pore system

[b] Number of tetrahedral atoms in their largest ring

[c] Three-letter code given by IZA [2, 3].

* Structure having extra micropore(s) with lesser number of tetrahedral members (10R or 8R). For details [2, 3].

[d] Common names. The name following the format 'AlPO$_4$-n' is preferred.

[e] The term 'None' indicates the possibility to prepare the material in the non-doped AlPO$_4$ form.

[f] Structure directing agent or any other strategy used in the preparation of the material. The term 'None' indicates the possibility of preparing the corresponding material in the absence of any SDA.

Organic SDA abbreviations: DPA: n-dipropylamine; TBAOH: tetrabutylammonium hydroxide; TEA: trimethylamine; TEAOH: tetrabutylammoniun hydroxide; TPA: tripropylamine; TPAOH: tetrapropylammonium hydroxide; MCHA: N-methyldicyclohexylamine; DBA: n-dibutylamine; DPentA: n-dipentylamine; DHA: n-dihexylamine; HMI: hexamethyleneimine; ECHA: N-ethyldicyclohexylamine; DPBA: N,N-diisopropylisobutylamine; DiPA: diisopropylamine; DiPFA: diisopropylformamide; DEA: diethylamine; DiBA: Diisobutylamine; HMTA: Hexamethylenetetramine; HMI: Hexamethyleneimine; MDEA: N-methyldiethanolamine; DDO: N,N´-dimethyl-1,4-diazabicyclo(2.2,2) octane dihydroxide; TMAOH: Tetramethylammonium hydroxide; DAN: 1,9-diaminononane; DMAP: 2- or 4-dimethylaminopyridine; MA: methylamine; DMA: dimethylamine; DEDMA: diethyldimethylammonium; ETMA: ethyltrimethylammonium; EA: Ethanolamine; PA: n-propylamine: MEA: N-methyl-ethanolamine; TrOH: Tropine hydroxide; DABCO: Triethylendiamine; MCA: 2- methyl-cyclohexylamine; DET: diethylenetriamine; DMOH: decamethonium hydroxide; BMP: (S)-(-)-N-benzylpyrrolidine-2-methanol; BP: benzylpyrrolidine; DAH: 1,7-diaminoheptane; TTD: 4,7,10-trioxa-1,13-tridecane diamine; DiPE: N,N-diisopropylethylamine; PDA: 1,3-propyldiamine; iPA: isopropyamine; tBA: tert-butylamine; TMHD: N,N,N′,N′-tetramethyl-hexane-1,6-diamine; EDA: ethylenediame; 1,2-DAP: 1,2-diaminopropane; Q: quinuclidine; NPA: neopentylamine or 2,2-dimetil-1-propanamina; CA: cyclohexylamine; DACH: 1,4-diaminocylcohexane; DiPPD: N,N'-diisopropyl-1,3-propanediamine; BQNB: 1,4-bis-N-quinuclidiniumbutane; tmtact: 1,4,8,11-tetramethyl-1,4,8,11-tetraazacyclotetradecane; hmhaco: 1,4,7,10,13,16-hexamethyl-1,4,7,10,13,16-hexaazacyclooctadecane; EMIM: 1-methyl-3-ethylimidazolium; MEDA: N-methylethylenediamine.

1.4 Heteroatoms incorporable into AlPO$_4$ frameworks and their structure-directing role

In an all-silica zeolite framework, all atoms in the tetrahedral coordination are tetravalent Si^{4+}. That Al-free zeolite is hydrophobic and does not have any overall charge. Practically all applications of zeolites are based on the partial substitution of Si by other heteroatoms, which provide acid/redox centres, basicity, hydrophilicity, ion exchange capacity, etc. The isomorphic substitution of a Si^{4+} by a tetravalent ion such as Ti^{4+}, Zr^{4+} or Sn^{4+}, does not alter the neutrality of the framework. However, the incorporation of Al^{3+} ions isomorphically substituting Si^{4+} entails the introduction of a negative charge, which has to be compensated by a cation, commonly a protonated SDA molecule, a proton H$^+$, alkaline or alkaline earth cations. Similarly, the incorporation of a pentavalent ion, for instance P^{5+}, would positively charge the framework and the presence of an extraframework anion would be required. To the best of our knowledge, the latter substitution (P or any other pentavalent ion by Si^{4+} one) has not been reported in the literature. In this sense, it has been noted that introduction of phosphate ions in the zeolite MFI synthesis gel seems to assist the crystallisation process but no evidence for P incorporation has been seen [60]. The incorporation of divalent atom instead of a Si^{4+} ion has been also attempted, but either two monovalent extraframework cations or a divalent one must be present to compensate the double charge of the framework associated to the incorporation of a divalent ion. In spite of the incorporation of divalent cations in zeolites has been described

Commented [ms3]: **Joaquín commented:** The framework is charged at local sites, as both Si and O bear some charge.
Answer: We agree

[61-64], this is far from being a widespread strategy, and the heteroatom incorporation in zeolites is reduced, for practical purposes, to tri- and tetravalent ions.

Since the aluminophosphate framework consist of alternating P^{5+} and Al^{3+} ions, the possible oxidation states of the incorporated heteroatoms are significantly expanded. Figure 3 shows various mechanism of substitution (MS) of heteroatoms, as well as the subsequent charge modification of the framework, if any, as a function of the oxidation state, covering from 2+ to 5+ ions, which are in principle easy to be achieved in an $AlPO_4$ framework, contrasting with the limited oxidation states within a SiO_2 framework (3+ or 4+, Table 1). Similar to the divalent heteroatom incorporation in zeolite framework that has been described in some particular cases [61-64], the incorporation of monovalent ions into $AlPO_4$ frameworks has also been claimed [65, 66].

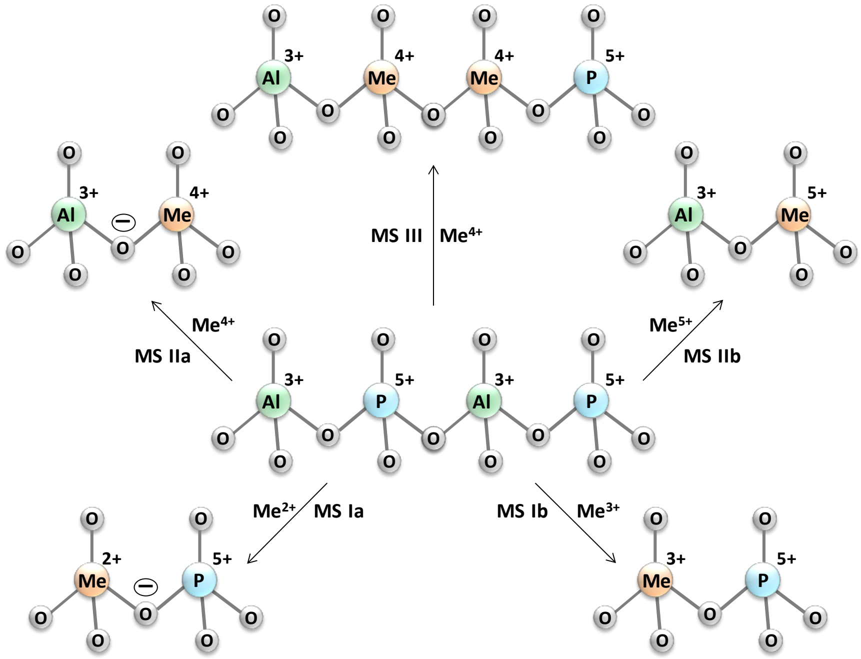

Figure 3. Mechanisms of substitution of heteroatoms with oxidation states 2+, 3+, 4+ and 5+ into an $AlPO_4$ framework.

Apart from the evident improvement in terms of versatility of incorporable oxidation states, Figure 3 makes clear that two further important distinctions are found in AlPOs in comparison with zeolites. Firstly, the incorporation mechanisms of a given heteroatom (and then also its final environment within the $AlPO_4$ framework) cannot be always predicted by just knowing their oxidation state. This is particularly true for tetravalent ions, which can provide up to three different incorporation mechanisms (MS IIa, MS III and the substitution of Me^{4+} by Al^{3+} ions, which has not been considered in Figure 3 because its existence has not been proved in AlPOs) or a combination of them in different degree. Such MS variety for tetravalent ions has been developed by Si^{4+}, giving rise to very different environments including isolated Si (by MS IIa) and a notable variety of SiO_2 islands (by combination of MS III and MS IIa mechanisms) (Figure 4). The environment of each Si atom shown in Figure 4 has strong influence on its acidity and then on its catalytic potential. Any incorporated Si surrounded at least by an Al atom in the first tetrahedral coordination sphere gives an acidic site. The acidity of these sites increases in the order: $Si(OSi)_3(OAl) > Si(OSi)_2(OAl)_2 > Si(OSi)(OAl)_3 > Si(OAl)_4$ [67], the latter being formed by the isolated incorporation of a Si^{4+} ion substituting a P^{5+} ion (MS IIa, Figure 3). So, the whole acidity of the SAPO catalysts (number and strength of their sites) with a given Si content is controlled by the size of the SiO_2 islands [68]. On the contrary, Si^{4+} atoms in $Si(OSi)_4$ environments within zeolite-like SiO_2 islands have no acidic properties at all; therefore, one may consider the incorporation of such Si^{4+} as heteroatom is useless as they do not provide any net catalytic site, although they can catalytically contribute in some other ways such as to increase hydrophobicity of the catalyst [69], to tune the acidity of other acidic Si sites beyond the isolated Si sites $Si(OAl)_4$ [42] or to improve thermal stability of the material [66]. Despite that diversity of environments has been exclusively attributed to the Si^{4+} ion during decades, the recent certification of the existence of Ti-O-Ti in TAPO materials [71] evidenced that such incorporation complexity is extendable to other tetravalent dopants.

Secondly, irrespective of its oxidation state, the incorporation of a given heteroatom ion has different consequences in terms of framework charge of zeolites and $AlPO_4$ zeotypes. For instance, if the incorporation of trivalent heteroatoms is the normal way to introduce charge (and then acidity, hydrophilicity, etc.) in zeolite frameworks, the same heteroatom incorporated into AlPOs does not alter the neutrality of the framework. It implies that the incorporation of a given heteroatom is never strictly comparable in both frameworks, as different breaking and/or preserving of neutrality will be certainly found in both systems.

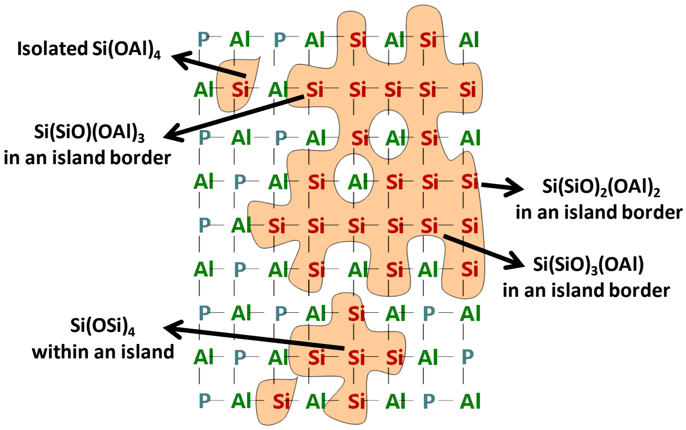

Figure 4. Different Si environments in an $AlPO_4$ framework formed by diverse combinations of heteroatom incorporation mechanisms MS IIa and MS III (Figure 3). The orange regions indicate the Si islands. Oxygen atoms, which are present between two consecutives tetrahedral atoms (P, Al or Si), are omitted for clarity.

Whilst previous sections showed the importance of organic structure directing agent or pH of the starting gel in directing specific structures, it is also reported in literature that certain incorporated heteroatom ions along with the SDA can direct specific microporous structures. This is particularly true for $AlPO_4$-based materials as illustrated in Figure 5. It has been found that 1,2-diaminocyclohexane produces a highly crystalline layered material in the absence of any divalent cations that substitutes Al^{3+}. However, the introduction of *ca*. 30 % of divalent metal ions in Al^{3+} sites, in particular cobalt or zinc, produces a material with chabazite structure [72]. Likewise, 1,4-diaminocyclohexane, which produces a layered material very similar to that formed from 1,2-diaminocyclohexane in the absence of any dopant, promotes the formation of a three dimensional microporous materials with PHI structure when a divalent metal ion such as Co^{2+} or Zn^{2+} is introduced in the synthesis gel [72]. It has been also observed that the heteroatom cation concentration can tilt the formation of CHA over AEI structure (both having highly related topologies [2, 3]) when TEAOH is used in conjunction with Co^{2+} ions in the synthesis gel [73]

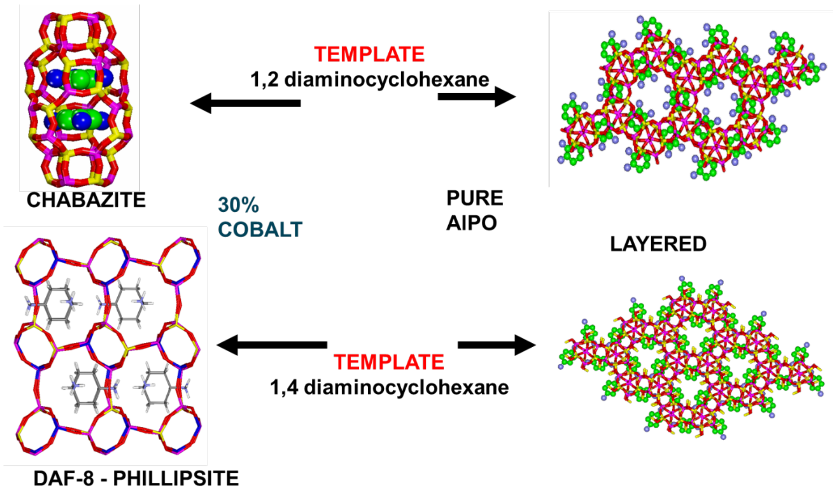

Figure 5. Effect of the presence of divalent ions Co^{2+} in tilting the structure direction from a layered $AlPO_4$ material to a 3D microporous Co-doped aluminophosphates system.

Other strong structure-directing role by an ion is found in the system AFI/CHA in the presence/absence of Zn^{2+} ion, whose role has been clarified through molecular interactions [52]. Similar effect has been also observed under ionothermal conditions, in particular by the presence of either V (introduced as V^{3+}, V^{4+} or V^{5+}) or Ti^{4+}ions, which favour the crystallization of CHA-structured materials to the detriment of AEL ones [74].

These examples and many others in the literature make clear the outstanding structure-direct effect given by certain heteroatom ions in the $AlPO_4$ systems, generally characterized by a low phase-specificity. Since this section focuses on the distinctness of zeotypes AlPOs versus zeolites, it must be highlighted that some heteroatom ions also possess a notable capacity to direct the formation of zeolites with particular structures. In this aspect, two of the most relevant ions are Ge^{4+} [11] and Zn^{2+} [61-63].

1.5. $AlPO_4$ topologies: the abundance of 1-D pore systems

$AlPO_4$-based microporous materials with around 50 different topologies have been prepared (Table 2). Therefore, the versatility is more than acceptable, considering that they cover all range of: (i) microporosity, as there are AlPOs with small pores (channels of 8-membered rings, 8R), medium pores (10R), large pores (12R) or extra-large pores (> 12R); (ii) pore dimensionality, with 1D, 2D or 3D pore systems; and (iii) the presence of either simple pores or pores plus (super-)cavities [2, 3]. In addition, there are so many topologies able to be prepared as AlPOs and as zeolites, which allows comparison and systematic studies. Even though, the versatility is far from reaching that of zeolites, since more than 230 topologies of the latter have been described and accepted by IZA [2, 3].

On the other hand, the non-doped $AlPO_4$ materials have marked tendency to crystallize as 1D-pore topologies. In particular, among the topologies prepared so far as pure $AlPO_4$ (which are marked as "None" in the column 'Incorporated Me' in Table 2), 40 % of them has unidirectional pore systems. It must be noted that only 25 % of the known zeolite frameworks has 1D pore system [2, 3]. Moreover, the most investigated $AlPO_4$-based materials, $AlPO_4$-5 (AFI), $AlPO_4$-11 (AEL) and VPI-5 (VFI), possess such pore arrangement and can be prepared with so many organic SDAs. Then, one can deduce that the phase specificity of these SDAs is quite weak. Indeed, VPI-5 can even be prepared without any organic SDA [75] as water molecules arranged in a triple-helix act as the real structure directing agent [76]. When amines or quaternary ammonia are added to the synthesis media, they would have certain role in the nucleation/crystal growth processes (mainly through pH control) but they are not found within the large (18R) VFI pores, indicating their negligible templating role [30]. The presence of heteroatom ions having certain structure-directing role often favours the formation of 3D-topology MeAPO materials versus 1D-topology ones, as above explained [72-74]. It must be also highlighted the difficulty of preparing zeolitic materials having these topologies: AEL and VFI has not been described whereas the AFI structured zeolite SSZ-24 was described after the discovery of $AlPO_4$-5. In the same sense, the preparation of non-doped $AlPO_4$ materials having typical zeolite structure with 3D pore systems is rather hard. The emblematic FAU topology in zeolites has only been prepared as $AlPO_4$-based form when they are doped with Si^{4+} [77], Co^{2+} [78, 79] or Zn^{2+} [79] and using a combination of SDAs, whereas the highly demanded CHA-structured SAPO-34 materials due to the use of SAPO-34 in MTO process [32], can only be prepared as pure $AlPO_4$ under very restrictive conditions including the use of HF [17, 80]. Nevertheless, it must be pointed out that these two low-dense cage-contained zeolites FAU and CHA are also difficult to be prepared in the non-doped SiO_2 form [81], suggesting that their preparation is favoured by the negative charge of the framework irrespective of their silica or aluminophosphate composition.

Commented [ms4]: **Joaquín commented:** The difficulty in preparing ALPO versions of these 3D zeolites is more related to the charge of the framework than to the 3D pore architecture. All-silica FAU is also unknown, and it is very difficult to prepared all.-silica CHA, which requires a proper combination of SDA. I believe the difficulty is more related to the preparation of neutral structures having low-density, as 3D structures usually have low-density. It could be convenient that you discuss this aspect.
Answer: We agree with your comment. We have added a new sentence. In our opinion, deepening this topic further is beyond the scope of this chapter.

From a catalytic point of view, topologies with 1D pore systems possess inherent drawbacks when compared with the 3D ones, due to both the diffusional problems of chemicals [82] and the quicker deactivation of the catalysts [83] found in the former. Fortunately, the introduction of heteroatom ions to lead MeAPOs increases the percentage of 1D topologies to that found for zeolites (Table 2).

2. General aspects of the synthesis of AlPOs

Almost all microporous aluminophosphates based systems are synthesised using an organic structure directing agent (SDA) (Table 2). In a typical synthesis appropriate stoichiometric amounts of aluminium source (aluminium hydroxide hydrate and pseuboehmite are two of the most popular sources but other aluminium compounds such as aluminium isopropoxide have also been investigated), phosphoric acid, water, metal salts if necessary and the SDA are taken and mixed in a specific order to create a gel; the order of addition needs to be optimised for specific synthesis of a given structure and composition. Similarly, the pH of the gel needs to be adjusted to obtain phase pure, specific structure. The prepared gel is introduced in a Teflon-lined autoclave and heated to specific temperatures for several hours to days depending on the system. A typical schematic diagram showing the general approach used in microporous aluminophosphates synthesis is shown in Figure 6. A selection of aluminophosphates based systems as well as the SDAs used to produce them is listed in Table 1. It has been noted that, although SDA is used for producing specific structured material, in many instances, other structures are favoured depending on the pH of the starting gel, temperature and time of reaction. Even the co-crystallization of more than one $AlPO_4$-based is quite often. Figure 7 shows a representation of such effect based on different systematic studies [84-86].

Commented [ms5]: **Joaquín commented:** This a well-known procedure. I think it is not necessary to include it in this kind of publication.
Answer: Fine. We have removed it.

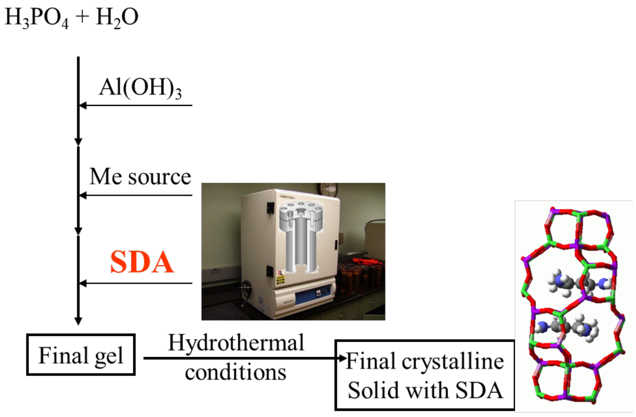

Figure 6. A schematic diagram of a typical synthesis of (heteroatom-doped) aluminophosphates material. SDA-Structure directing agent, typically an organic amine or ammonium hydroxide templates. Macrocycle based metal complexes and multi-templating approaches have also been used in many cases [86, 87].

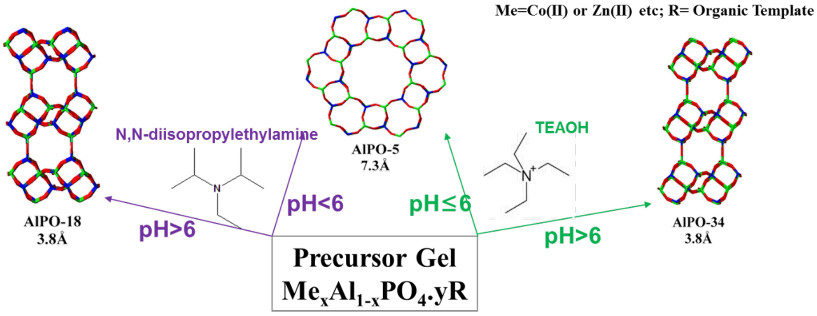

Figure 7. Scheme of the competitive formation behaviour of two structures that are formed using the same template and temperature. The control of pH of the starting gel is shown to be important to produce specific structure [85, 88].

3. Characterization of the metal sites incorporated within AlPOs

To characterise aluminophosphates in general and heteroatom-substituted systems in particular, a range of techniques are used. The main reason of such variety of available characterisation methods are: (i) the complete characterization of a solid (catalyst) includes so different aspects as crystalline structure, chemical composition, chemical/thermal stability, porosity, surface area, chemical environment of Al, P and dopants, morphology crystal size, acidity/redox strength, etc.; (ii) the AlPO$_4$-based materials possess great variety in terms of topology and composition; (iii) the active centres used to be the dopant, whose loading is normally quite low; (iv) the different characterization techniques give complementary information; and (v) each technique has some limitations.

3.1. Structural characterization

As these materials are highly crystalline with ordered arrangement of atoms, X-ray diffraction is the primary technique used to determine (a) phase purity of the prepared systems, (b) lattice parameters (by simple Rietveld analysis using a method known as Le Bail method) and (c) complete structure solution using Rietveld analysis by providing an initial structure and refining structural parameters such as atom positions, occupancies, temperature factors etc. to obtain a best match between experimental and calculated diffraction pattern from the refined structure [89-92]. In some cases, when the initial structure is not available or not well-defined, many other combination of methods, in particular molecular modelling methods or electron microscopic methods were used to provide initial structural information and further refined using powder diffraction data to obtain more accurate structures of the synthesised materials

[90, 93-96]. Whilst powder diffraction is used routinely as obtaining well defined single crystals of certain size is difficult in many aluminophosphates systems, in some instances single crystals could be obtained and hence single crystal diffraction methods can be used. With advent of micro-crystal diffraction methods it is now possible to obtain high-quality data of crystals as small as 10 microns or less in a Synchrotron Radiation source [97]. At the same time, one grain in a large batch of sample with a crystal used for structure solution may not provide the confidence that entire powder has the same material and structure. It is best to carry out powder diffraction of the same material with multiple crystalline parts and use the structure obtained from Single crystal diffraction as the starting structure to ensure the entire powder can be modelled with this structure. Figure 8 shows the structure obtained from combined single crystal and powder diffraction of the same DAF-5 material (CHA structure, synthesized using a computationally determined SDA, 4,4, piperidinopiperidine) proving that entire powder pattern can be modelled with the structure determined from single crystal diffraction [98]. Powder diffraction of the as-synthesised materials alone is not sufficient as it is required to calcine the material to remove the organic template for many applications. Therefore, it is strongly recommended to carry out powder diffraction of calcined material to ensure the structure has not changed in the process of heating the sample. Ideally, one should use *in situ* methods or to avoid exposing the calcined material to atmosphere (dry state) to prevent any post calcination interactions with atmosphere, especially water molecules, as these materials are hydrophilic and this interaction can distort the structure of calcined material.

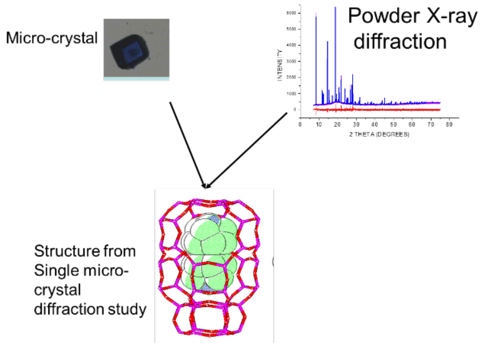

Figure 8. Scheme structure solved using micro-crystal diffraction methods using station 9.8 at Daresbury laboratory and subsequently verified using high-resolution powder diffraction recorded at station 2.3 at Daresbury laboratory of DAF-5, a CoAPO-34 material synthesised using computationally designed organic SDA [98].

Commented [ms6]: **Joaquín commented:** The PXRD is so small that the figure is useless in this size.

Commented [ms7]: Sankar, could you modify the figure in the sense Joaquín suggested?

Although X-ray diffraction provides unique structural details, in particular atomic-architecture, pore distribution, template location and in some cases if the hetero-atom is ordered enough their possible site location and occupancies, often the technique fail to produce the location of hetero-atoms located in the T-site. Some of the reasons are that they may not be ordered and also that in the majority of the cases, the concentration of the metal ions is too small to show any effect. However, Simmance et al. [99, 100] indeed show that there are specific lattice expansions in certain directions, in cobalt and zinc substituted aluminophosphates. Despite this observation, it is difficult to determine the local structure of the substituted metal ions unless a more specific local structural tool is used, specifically adaptable to systems with low concentrations of heteroatoms. NMR is ideal, but accessing such nuclei is difficult. X-ray absorption spectroscopy is another preferred technique as it is a local structural technique and element specific, which is discussed later

3.2. Characterization of heteroatoms incorporated in $AlPO_4$ frameworks

High-resolution solid-state ^{27}Al and ^{31}P NMR have been extensively used to understand the local environment of the framework and extra-framework ions. However, most of the studies are limited to pure $AlPO_4$ materials or those doped with non-paramagnetic heteroatom ions, like Si^{4+}, Mg^{2+} or Zn^{2+}. The presence of paramagnetic dopants does not only avoid the NMR-based study of the heteroatoms themselves but it also avoids to study the sample itself. In spite of significant effort made by Tuel et al. [101, 102] recording ^{31}P NMR spectra over an extended acquisition window, this technique is far from being able to be applied routinely in conventional laboratory based NMR instruments. They detected different $P(Co_n,Al_{4-n})$ $(0 \geq n \geq 4)$ environments separated by several thousands of ppm. Moreover, among the diamagnetic (non-paramagnetic, able to be studied by NMR) heteroatoms, just a few of them, such as Si^{4+}, Sn^{4+} or Cd^{2+}, possess isotope with good enough NMR sensitivity or natural abundance to be able to be studied by this spectroscopic technique. However, in most cases, the low loadings of hetero atoms in AlPOs, critically limit the acquisition of good signal-to-noise NMR spectra. In practice, just ^{29}Si NMR spectra have been used to directly detect the different heteroatom (Si) environments in Si-substituted AlPOs. Other important diamagnetic heteroatoms, from a catalytic point of view, in particular Mg^{2+}, Zn^{2+} or Ti^{4+} have very poor sensitivity to NMR, but their incorporation mechanisms or their chemical environment into the $AlPO_4$ frameworks can be indirectly studied by solid-state ^{27}Al and especially ^{31}P NMR [103-106].

Some metal ions containing AlPOs, in particular those containing cobalt and manganese, changes their colour when the oxidation state of the metal changes. In this sense, UV-vis spectroscopy could be an ideal technique for studying these systems [107-114]. For example, cobalt substituted system CoAPO-36 was studied using this technique and the colour change from blue (as synthesised) to green (in the calcined and oxidised form) was used as evidence

Commented [ms8]: **Joaquín commented:** What kind of structure?
Answer: It has now been mentioned.

for the formation of Co^{3+} upon calcination in air [110]. Weckhuysen et al. reported a 30% conversion of Co(II) to Co(III) [115] which is line with the findings reported by Barrett et al. [116] using Co K-edge EXAFS technique, discussed later. A representative spectrum is shown in Figure 9 which shows as-synthesised, calcined and reduced forms of CoAPO-5.

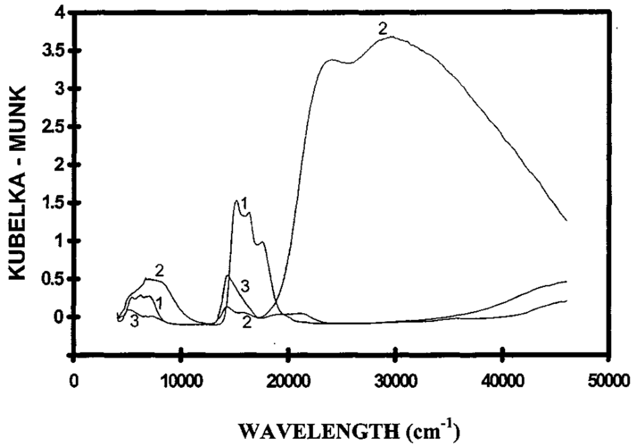

Figure 9. DRS spectra of CoAPO-5 materials as a function of the pre-treatment: (1) in as-synthesized form; (2) after calcination overnight at 773 K and (3) after reduction with H_2 at 623 K. Reprinted from Zeolites, 19, A. A. Verberckmoes et al., Framework and extra-framework Co^{2+} in CoAPO-5 by diffuse reflectance spectroscopy, 180-189, Copyright 1997, with permission from Elsevier [111].

Fourier Transform Infrared spectroscopy has been very useful in characterising a range of heteroatom substituted system for two reasons: (a) if the metal ions are present in a lower valence state (whether it is 2+ in Al^{3+} site or 4+ in P^{5+} site) a charge compensating proton should be present resulting in a bridging hydroxyl, which will have a specific OH stretching frequency, similar to the one seen in zeolitic solids and different from terminal hydroxyls associated with parent Al^{3+} or P^{5+} cations. A characteristic band appears around 3600 cm^{-1} associated with bridging hydroxyls when divalent metal ions are present [117-119] (Figure 10). This method is routinely used in addition to proton NMR (if non-paramagnetic metal ions are present) in selected heteroatom substituted aluminophosphates (in completely dehydrated form) to establish the presence of Brönsted acidity in these systems. However, it is difficult to use this method to establish the extent of conversion of transition metal ions (example Co^{2+} to Co^{3+} upon calcination) as the intensity of the OH is not clearly reflected on the extent of

Commented [ms9]: **Joaquín commented:** As it is written, this sentence seems to suggest that this band can be seen in all the materials substituted with divalent ions. Hence, you should discuss this point, or refer in the text to the specific Co-materials were this band has been observed.

Sankar, I prefer you to answer this question and, if required, to modify the text.

conversion and furthermore, it is difficult to deduce the presence of Lewis acid sites unless a probe molecule is used to determine the Brönsted and Lewis acid sites.

Commented [ms10]: **Joaquín commented:** Please clarify this sentence.

Sankar, can you reply to this comment by Joaquín?

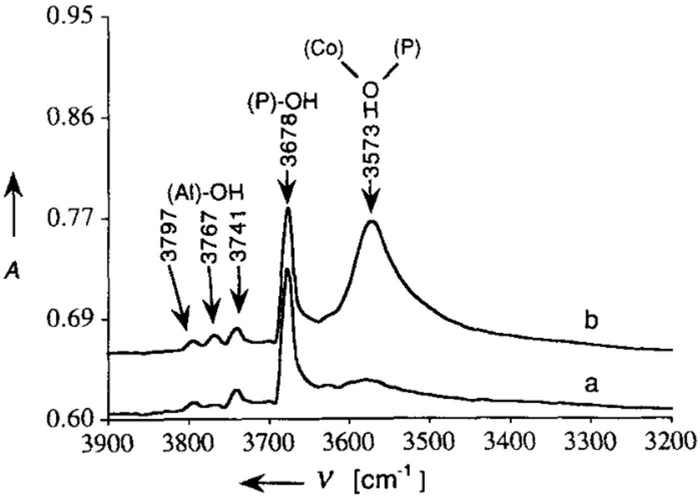

Figure 10. IR spectra showing OH stretching vibration mode of CoAP0-18. a) Calcined in oxygen at 550 "C, b) reduced in hydrogen at 400 ºC. A = absorption. Thomas JM, Greaves GN, Sankar G, Wright PA, Chen J, Dent AJ, Marchese L: On the nature of the active site in a CoAPO-18 solid acid catalyst. Angew. Chem. Int. Ed. 1994, 33, 1871-1873. Copyright Wiley-VCH Verlag GmbH & Co. KGaA. Reproduced with permission. [119].

Extensive studies using ESR technique were conducted on a range of transition metal ions substituted AlPOs [115, 120-129]. Although it was established by a range of techniques that 2+ ions substitute for Al(III), some of the results were interpreted in such a way that the metal (2+) ions may substitute for P(IV) site instead of Al(III) sites. Although it is possible, in such an event, a large number of protonated sites (almost 3 times as that of the 2+ ions substituted in 3+ sites) are needed for charge compensation. Therefore, as there are no direct proofs that such mechanism existed, one can most probably discount such substitution mechanism due to the nature of charge compensating species. Beale et al. [130] carried out ESR studies of cobalt and manganese containing aluminophosphates. They investigated both as-synthesised and calcined materials (the samples were sealed in vacuum after the calcination treatment in an ESR compatible tube). This study indeed supports the substitution of Mn (II) and Co(II) in the Al(III) sites in the as-synthesised materials and the formation of 3+ ions upon calcination [130].

X-ray absorption spectroscopy is a powerful method as it is element specific and provide average oxidation state and coordination environment (qualitatively) from X-ray absorption near edge structure (XANES) and coordination number and bond distance (local structure) more quantitatively from the analysis of the extended X-ray absorption fine structure (EXAFS). As this technique does not suffer from the lack of concentration of the dopant and irrespective of whether the material is crystalline or amorphous, it can be used for estimating the nature of substitution of the metal ions. A range of reports in literature utilised this technique and reported the substitution of 2+ metal ions in the framework and has become a routine method to convincingly establish the metal ions substitution. One of the main reasons that this method is required is that the diffraction analysis fails to show the presence of metal ions in their analysis as the metal ions are not ordered and furthermore, their concentration is fairly low. In addition, the majority of the AlPOs and MeAPOs (where Me is a divalent cation) possess high symmetry space group in diffraction analysis and have only one or two crystallographic sites which prevent the accurate determination of metal ion location. Barrett and Jones [97] used resonant scattering X-ray diffraction method to show that there is an unequal distribution of Co(II) in two Al(III) sites in DAF-8 having Phillipsite structure. A systematic study by Barrett et al [72] revealed that the extent of oxidation state change based on the metal-oxygen distance as the ionic radii of the different oxidation states and coordination numbers are different (Table 3).

Commented [ms11]: **Joaquín commented:** The concentration of the dopant also affect the measurement. May be the sentence can be rewritten.

Sankar, can you reply to this comment?

Commented [ms12]: **Joaquín commented:** This sentence is a repetition of what has been said in the previous one.

Sankar, can you reply to this comment?

Table 3. Refined occupancy of Al and Co sites in the 4 tetrahedral (T) sites wherein Al and Co occupy in DAF-8 material. Respective average distances of those sites agree with the percentages estimated in their occupancies. Typical distances of cation-oxygen distances for Al-O is 1.73 Å and for Co-O is 1.94 Å [72].

Crystallographic position T	% Al occupancy	% Co occupancy	Average Bond length M-O (Å)
T1	70.5(10)	29.5(10)	1.779
T2	42.2(10)	57.8(10)	1.843
T3	35.1(10)	64.9(10)	1.879
T4	73.9(10)	26.1(10)	1.780

It emerged that some structures favour a higher degree of redox reaction of Me(II) ions compared to others. For example, AFI structure seems to show the least of Co(II) ions present in its framework that can be converted to Co(III) compared to CoAPO-34 or CoAPO-18 systems. However, for Mn(II) substituted system, although the trend appears to be similar to that of cobalt, it is found that higher amounts of Mn(II) are converted to Mn(III) in AFI structure, compared to cobalt containing AFI material (Table 4) [116, 131].

Commented [ms13]: **Joaquín commented:** Under which conditions?
Answer: Sankar, could you reply to this question?

Table 4. Amount of 3+ ions present in the calcined state, at room temperature, under inert dry conditions, estimated from the average metal ion – oxygen distance estimated from EXAFS at the respective metal (Co or Mn) K-edges.

System	Average Me-O distance in the as-synthesised state (Å), R_{2+}	Average Me-O distance in the calcined (oxidised) state (Å), R_{av}	Amount of Me ions 3+ state (percent)^{a}- X(%)

CoAPO-5	1.94	1.91	23
MnAPO-5	2.02	1.92	58
CoAPO-36	1.93	1.86	58
MnAPO-36	2.02	1.89	76
CoAPO-18	1.93	1.82	100
MnAPO-18	2.02	1.85	100

[a] The amount was estimated based on the equation $X(\%)=(R_{av} - R_{3+})/(R_{3+}-R_{2+})$. R_{3+} was obtained based on the ionic radii displayed in Shannon ionic radii table – O^{2-} = 1.35, Co^{2+} = 0.58 and Mn2+=0.66. Both Mn^{3+} and Co^{3+} are not listed as it is very difficult to stabilise them in tetrahedral coordination. Therefore, the calcined state in MeAPO-18 was taken as the evidence for Me^{3+}-O distance as the edge shift in respective X-ray absorption data, correspond to 3+ containing model compounds. Therefore, Co^{3+}-O distance of 1.82 Å and Mn^{3+}-O distance of 1.85 Å were taken as representative distance for tetrahedrally coordinated Me^{3+}-O distance. The values are reported in refs. [116, 131]

Based on these studies a simple picture emerged on the extent of oxidation of, for example cobalt substituted aluminophosphates. A schematic model based on the amount of oxidised cobalt present in the system and the nature charge compensation in the case of non-oxidized cobalt ions in the framework is proposed by Barrett et al. [116] and shown in Figure 11.

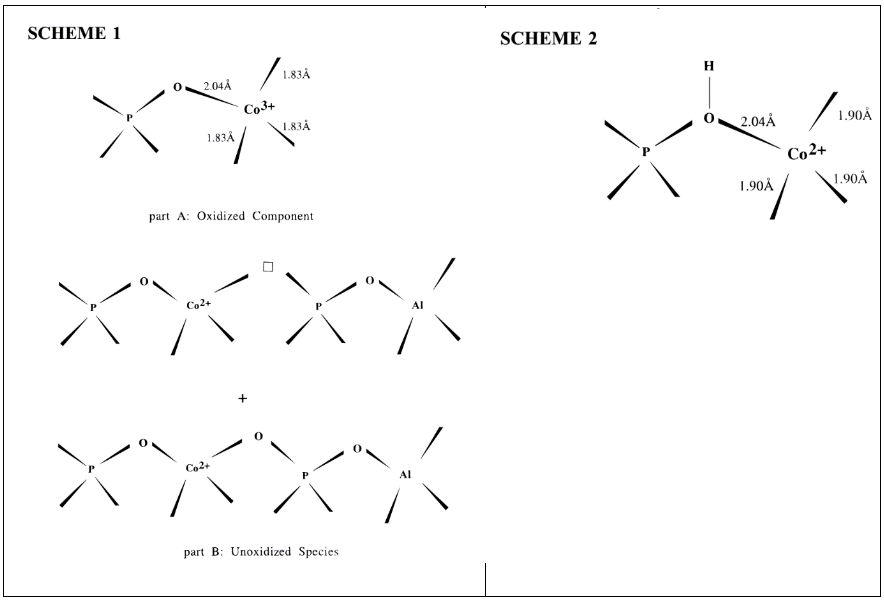

Figure 11. Schemes proposed based on results from EXAFS study at the cobalt edge of a series of CoAPOs in the calcined state and reduced state, taking in to account the oxidised and non-oxidized component (Scheme 1) estimated from EXAFS in the calcined state and reduced component after reduction in hydrogen (Scheme 2). Reprinted with permission from [116]. Copyright 1996 American Chemical Society.

Commented [ms14]: **Jaoquín commented:** The equation is not clear to me. For Co-and MnAPO-18, if all of the ion metals are present as M3+, then Rav-R3+ = 0, and the amount would be 0, not 100%.

Commented [ms15]: **Joaquín commented:** This is a mistake, it should be R_{2+}

Sankar, please, can you reply to these two comments?

Commented [ms16]: **Joaquín commented:** This is in the caption to the figure.

In addition, a detailed time-resolved combined XRD/XAS (at the Co K-edge) investigation of CoAPO-18 revealed the pathway in which the template decomposition takes place accompanied by acid site formation prior to the conversion of Co(II) to the oxidised 3+ ions. Figure 12 shows a schematic structure of extent of oxidation present in a typical four different structures with identical cobalt concentration of ca 4% derived based on the in situ Co K-edge EXAFS and FTIR studies. Furthermore, the in situ XRD/XAS (XAS at the Co K-edge) studies indeed revealed that the overall structure of the material is intact during the calcination and reduction processes and more importantly the conversion of Co^{2+} to Co^{3+} occurs at ca 500 ºC whilst the charge compensating organic cations decomposes much earlier, suggesting that both the events are not related. The results based on the study of CoAPO-18 are shown in Figure 12.

Commented [ms17]: **Joaquín commented:** Only one structure is reported in fig. 12. Please rewrite the sentence, it is unclear.

Sankar, could you reply to this comment?

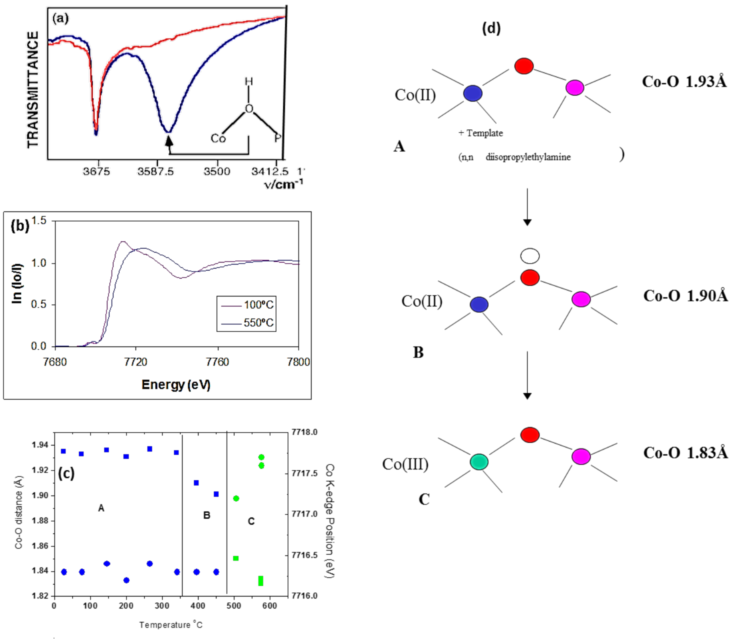

Figure 12. On the left, summary of the results obtained from a combination of XRD (not shown), FTIR spectra, Co K-edge XANES spectra and Co-O distance vs temperature of a CoAPO-18 material. One the right, the different Co environments at different experimental stages deduced from the results of the characterization techniques shown on the left: A) in the starting material, B) an intermediate structure when the SDA decomposes leaving a proton resulting in an acid catalyst, and C) the oxidised cobalt state that appears above ca 480 ºC.

4. MeAPOs as efficient catalysts

A range of catalytic studies have been undertaken to establish the performance of these metal ions substituted systems; the field is exhaustive and only selected reported applications are given here to demonstrate the use of these solids for a range catalytic applications. First and foremost studies focussed on the acid catalysed reaction of methanol to hydrocarbon. If metal ions are in 2+ state, there will be charge compensating protons (similar to aluminosilicate zeolites) and these are expected to catalyse the transformation of methanol to olefins. Indeed, several studies showed that the deactivation also appears to be an issue in some of these systems. Although these metal-containing systems shows performance for acid catalysed reactions, SAPO based systems were found to be superior [117, 122, 132-134].

The more promising area in the field of heterogeneous catalysis for metal ions substituted aluminophosphates is the selective oxidation of hydrocarbons utilising the redox reaction associated with the transition metal ions, in particular, cobalt, manganese, iron, vanadium and titanium based systems [135-144]. One of the examples in the field of hydrocarbon oxidation was the cyclohexane oxidation to alcohol, ketone and acid using metal substituted aluminophosphates materials. It was first shown that CoAPO-36, which has the appropriate large pore dimension for the cyclohexane molecule to enter into the structure and in addition fairly good conversion of Co(II) to Co(III) ions (based on EXAFS studies) showed a good conversion from cyclohexane to adipic acid under moderate temperatures of *ca.* 100 ºC and pressures of *ca.* 10 bar of oxygen/air [145]. The use of so environmentally benign oxidants is an extraordinary industrial advantage. Although EXAFS studies indicated that CoAPO-34 and CoAPO-18 8-R materials have almost all the Co(II) sites converted to Co(III) after calcination [116], the activity was very poor, which was explained as due to their small pore dimensions which prevent the entry of cyclohexane molecule (Figure 13).

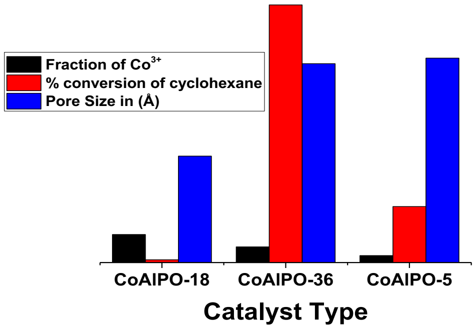

Figure 13. Comparison of the fraction of Co^{3+} formed upon calcination, as estimated by EXAFS (black column), the conversion of cyclohexane (red column) and the pore size of three CoAPO catalysts.

Therefore, further investigations were made on the effect of type of transition metal ions on the large pore $AlPO_4$-5 structure [36], as it can be prepared using a range of organic templates and relatively short time is required to produce these materials compared to $AlPO_4$-36 framework. It has been found that manganese and iron containing $AlPO_4$-5 structures, wherein the redox reaction for the conversion of 2+ ions to 3+ is facile compared to cobalt based systems, showed considerably higher activity for the conversion of cyclohexane (Figure 14).

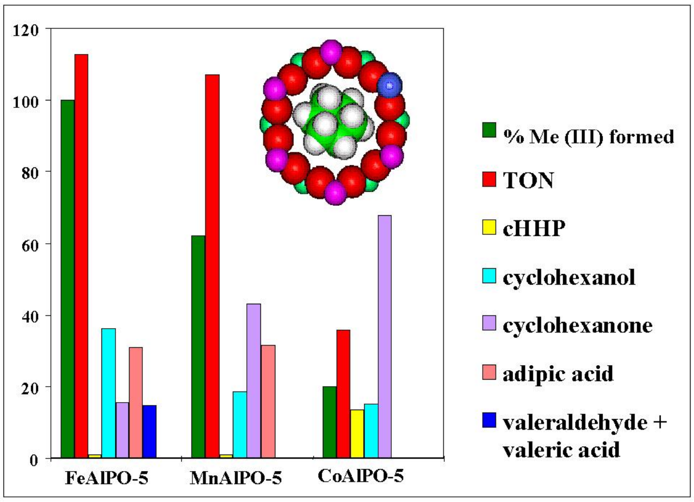

Figure 14. Conversion of cyclohexane to various products over three different metal ions (identical metal ion concentration of ca 4%) substituted $AlPO_4$-5. The red and green columns represent percent of M(III) ions present (estimated from EXAFS) in the calcined FeAPO-5, MnAPO-5, and CoAPO-5 and their catalytic activity (TON) for the oxidation of cyclohexane after 24 h at 403 K, respectively. Individual product distributions are also shown. Reprinted with permission from [36]. Copyright 1999 American Chemical Society.

The study also showed that introduction of free radical initiator, in particular tert-butyl hydroperoxide, enhanced the activity whilst the activity decreased considerably in presence of a radical quencher, such as hydroquinone.

Subsequent studies focussed on the oxidation of other inert hydrocarbons in particular linear molecules as they can access even to small pore AlPOs. Thomas and co-workers [35, 37, 146] showed that CoAPO-18 is an excellent system to oxidise selectively the end carbon of an n-hexane molecule as it has restricted entry through only one direction. With CoAPO-18 (and CoAPO-34) having much higher conversion of 2+ to 3+ ions during the catalytic activation, they exhibited a good regioselective oxidation of linear n-hexane molecule (Figure 15). Similarly, the manganese-containing small-pore materials also showed very promising

Commented [ms18]: Joaquín commented: Please check if the meaning of this sentence is correct

Sankar, it is better if you check.

selective oxidation of linear hydrocarbons. Whilst these studies established the ability of these small pores catalysts to restrict the molecular entry and regioselective oxidation (C1 in this case), there were reports in the literature on the nature of catalytic performance on these systems [138, 142]. However, this area of selective oxidation with redox metal ions substituted system is a promising field to explore in the future. Computational studies by Catlow and co-workers indeed provided a detailed mechanistic insight in to the path of the selective oxidation process that takes place in MeAPOs in oxidising alkane molecules with molecular oxygen. Specifically, these studies revealed that the catalytic efficiency of Mn-APOs in oxidation reactions is intrinsically linked to the Mn redox activity, in particular the interconversion between 2+ and 3+ oxidation states, and the coordinatively unsaturated nature of tetrahedral Mn present in AlPO frameworks. The proposed mechanism demonstrates the crucial role of both Mn-III and Mn-II in the reaction in which the Mn^{3+} sites (in the calcined form) undergo an initial reaction to form alkyl hydroperoxide intermediate, which is transformed into the oxidative products (alcohol, aldehyde and acid) by reduced Mn^{2+} [131, 147-155].

Commented [ms19]: **Joaquín commented:** What do the say?

Sankar, can you reply to this comment?

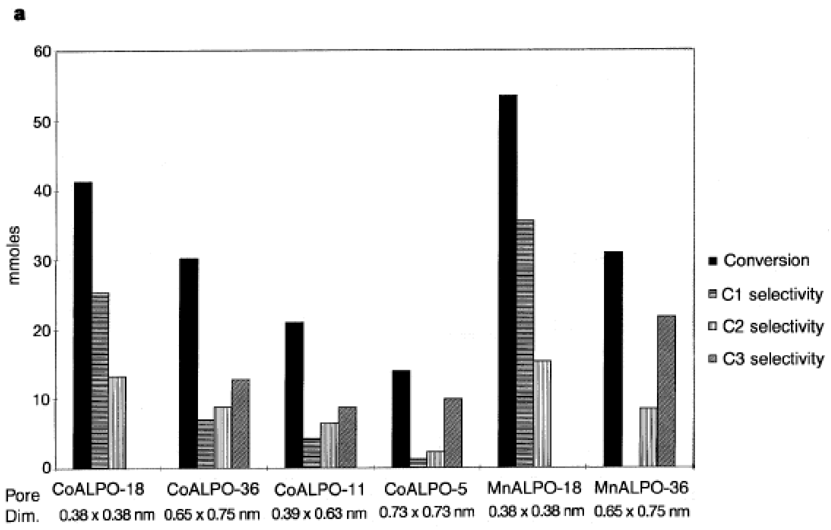

Figure 15. Comparison of catalytic oxidation of n-hexane in presence of molecular oxygen and cobalt or manganese substituted aluminophosphate molecular sieves. Selectivity towards the oxidation of C1 part of the n-hexane molecule is achieved in small pore material, primarily due to restrictions in the way the molecule can enter the small pore. In addition, both cobalt and manganese containing $AlPO_4$-18 have highest conversion of Me^{2+} to Me^{3+} and therefore shows good conversion compared to $AlPO_4$-5 or $AlPO_4$-11 or $AlPO_4$-36 structures. Reproduced by permission from Macmillan Publishers Ltd: Nature [35], copyright 1999.

It is also significant that the same kind of MeAPO catalysts, in particular FeAPO-5 and MnAPO-5, were reported to be active in the oxidation of cyclohexene under soft/mild conditions, in liquid phase, at 80 ºC and under ambient pressure, but using hydrogen peroxide as oxidant agent [156]. That activity was clearly overtook several year ago by the use of multi-transition-metal-doped $AlPO_4$-5 or MeAPO-5 (Me = heavy metal) catalysts [157], as it would be explained in detail in the next section. However, as a precaution under peroxide presence, one need to establish that metal ions are not leaching from the solid, which could be an issue which needs to be addressed in this and many other liquid-phase oxidation reactions.

Iron containing ZSM-5 was reported to be an efficient catalyst for the conversion of benzene to phenol using N_2O as an oxidation reagent. Whilst several studies were undertaken to understand this process, Shiju et al [158] explored iron substituted $AlPO_4$-5 as a catalyst for the same reaction through one-step calcination instead of steaming to extract some of the Fe3+ from the ZSM-5 framework. They reported a good activity for the conversion of benzene to phenol with a good selectivity for phenol comparable to FeZSM-5 catalyst (Figure 16). They investigated 3 different concentrations of iron and found that ca 1% of Fe in Al^{3+} site is sufficient to provide good activity and selectivity. Subsequent detailed study by Wei et al. [159] explained that N_2O did not decompose at the Fe^{3+} sites forming "alpha" oxygen similar to Fe-ZSM5 catalyst, instead, possibly undergone reduction from Fe^{3+} to Fe^{2+} by reacting with benzene and subsequently the oxidation takes place.

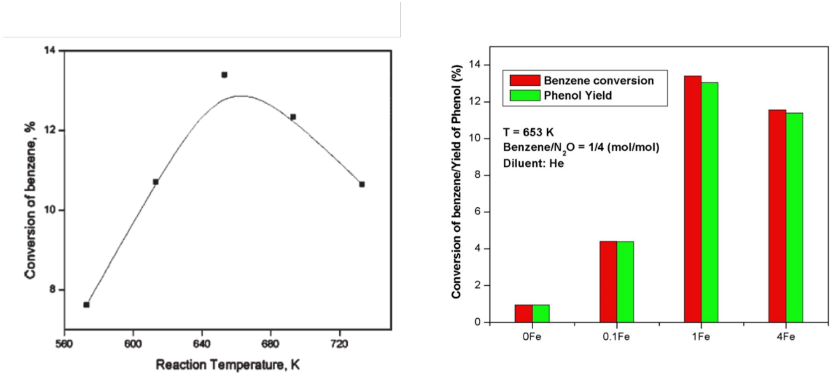

Figure 16. On the left, Catalytic activity of 1 wt. % FeAPO-5 as a function of temperature for the oxidation of benzene to phenol. Benzene : N_2O : He = 1 : 3.6 : 5.4, contact time factor = 0.5 s. Reproduced from ref. [158] with permission of The Royal Society of Chemistry. On the right, activity and phenol yield for various concentrations of iron substituted $AlPO_4$-5 material.

There are several other examples of a range catalytic studies reported with MeAPOs which include epoxidation of alkenes [160], Baeyer-Villiger oxidation [161], alkylation of benzene with aromatics by benzyl chloride over iron containing aluminophosphates [162], multifunctional MeAPO-5 catalyst containing a redox and non-redox metal ions for one-step conversion from cyclohexanone to caprolactam [163], liquid phase oxidation of styrene and synthesis of adipic acid from cyclohexanone using MnAPO-5 in presence of tert-butyl hydroperoxide [164], phenol hydroxylation over iron containing $AlPO_4$-5 prepared by hydrothermal methods, ion-exchange and impregnation methods for phenol hydroxylation and ethane oxydehydrogenation over MnAPO-5 [165].

5. Structure directing effect in MeAPOs: the importance of phase specificity in the design of improved catalyst

As it has been mentioned above (Table 1), the phase specificity is one of the main disadvantages of the synthesis of $AlPO_4$-based microporous materials in comparison with the preparation of zeolites. For instance, $AlPO_4$-5 or $AlPO_4$-11 materials can be prepared in the presence of tens of different amines but they only become pure under very narrow synthesis conditions. Similarly, several topologies with AlPO4 composition can be prepared for instance using n-dipropylamine (DPA) as SDA by just minimally changing certain parameters such as crystallization temperature, crystallization time, pH of the starting gel, dilution, order of addition of the reactants or the presence/absence of heteroatoms. The fact that a particular $AlPO_4$-based material can be prepared in pure form only under narrow conditions is particularly relevant for the subject of this Chapter, so it is addressed more in depth in this section.

Among the $AlPO_4$-based frameworks, it seems that some topologies are easy to be prepared as pure $AlPO_4$ composition, such as AFI ($AlPO_4$-5) or AEL ($AlPO_4$-11), whereas some others such as CHA ($AlPO_4$-34) or ATS ($AlPO_4$-36) are relatively easy to be synthesized in the presence of a heteroatom and extremely hard to be prepared in the Me-free $AlPO_4$ form [80, 166]. Some others scarcely investigated $AlPO_4$-based materials like AFY ($AlPO_4$-50), AFX ($AlPO_4$-56), AFV ($AlPO_4$-57), SAO (STA-1) or AFS ($AlPO_4$-46) have not been reported until today as non-doped AlPOs but they exist in their SAPO, MeAPO or MeAPSO forms (Table 2) [2, 3]. Indeed, almost half of the reported metal-substituted AlPOs has not been able to be prepared as AlPOs [167] (Table 2). A clear example is seen with AFI and CHA structures, as only AFI-structured materials is obtained from a non-doped aluminophosphate gel whereas the same gel containing Zn as dopant led to pure CHA phase ZnAPO-34 [52, 168]. Something similar happens in a ionothermal media with the topologies AEL and CHA [74], where the presence of V or Ti favours the crystallization of the latter to the detriment of the former, which is the only crystallized phase starting from heteroatom-free $AlPO_4$ mixtures. In other words, the structure directing role in AlPOs is not exclusive of the amines but the heteroatoms

Commented [ms20]: **Joaquín commented:** Do you mean that pure Al - P containing gels crystallize AFI?

Answer: Yes, we do mean that. In order to clarify the meaning of the sentence, it has been re-written.

themselves have a key effect on the phase specificity to certain topologies, suggesting the direct involvement of heteroatom ions in the formation of the first crystallization nuclei [52]. The series of Me-rich $AlPO_4$-based materials known as DAF-n [20, 72, 169], described in a previous section and that are not able to be prepared in the absence of Me, could be taken as the link between these $AlPO_4$-based materials preferably prepared in the presence of certain amount of metal ions and the Al-free zeotypes also based on phosphates [21, 27, 43].

Despite such involvement of heteroatom ions is in principle desired because it somehow guarantees the right incorporation of the metals within the $AlPO_4$ framework, it also entails a significant drawback in the design of systematic studies, for instance by varying the nature (and/or the loading) of the metal ion for a given structure. Using the same phase-specific organic SDA in this kind of systematic studies does not only guarantee the achievement of the same structure but it also makes practically equal other features of the resultant materials such as: (i) the (limited) number of metal ions to be incorporated as a function of the size and the number of charge of the SDA; (ii) the pH of the crystallization process, which influences on the possible hydrolysis of the heteroatom sources and on the subsequent formation of solid metal-rich impurities [47]; (iii) the crystal size, which could become the most critical parameter of these MeAPO materials when used as heterogeneous catalysts; (iv) the crystal morphology, particularly important in the 1-D topologies, which are abundant in the $AlPO_4$ family, etc.

For that goal, a suitable strategy is to enhance the phase specificity of the organic SDAs. In this sense, theoretical simulations can contribute in the design/prediction of more efficient organic molecules as templates for $AlPO_4$-based structures [170]. Even the following simpler strategy showed to be of great help.

The low structure-directing effect of amines in the synthesis of AlPOs generally dissuades of establishing a rational and direct correlation between the shape/size of the amines acting as SDA and the pores of the $AlPO_4$ topologies directed by them. Nevertheless, $AlPO_4$ family offers a series of quite systematic and simple topologies having 1D pore systems which crystallize in the presence of amines used as SDA [2, 3]. Taking the most common SDA amines NR_3 (where R represents the three substituent groups of N in an amine, and it can be -H, $-CH_3$, $-CH_2CH_3$, etc. depending of the nature of the amine) in their most thermodynamically favourable conformation, an acceptably good matching between the shape of the so-conformed amine and the shape of the $AlPO_4$ pore was found if the bulkiest R groups are positioned along the channel [171]. It suggests that amines have indeed certain templating role in the synthesis of microporous aluminophosphates, and they are not only pH modulator or simple pore fillers [172, 173].

As a proof of concept of this empirical model, several other amines scarcely studied by then in the synthesis of AlPOs were tested and led to either very important improvements in the specificity toward a particular topology or to the discovery of new amine-based SDA molecules for certain 1D pore $AlPO_4$ materials [171]. The following subsections focus on each of these two achievements by this rational-empirical method, specifically on the interest for incorporating heteroatom ions within the $AlPO_4$ frameworks.

5.1. N-methyldicyclohexylamine (MCHA), the by-far most specific SDA to an $AlPO_4$ material

a. MCHA as a phase-specific SDA for AFI-structured materials

The ease of preparing $AlPO_4$-based materials has strongly conditioned the choice of certain aluminophosphate structures to deepen their physicochemical knowledge and their subsequent applications. It does not seem a coincidence that: (i) $AlPO_4$-5 and $AlPO_4$-11 (IZA codes: AFI and AEL, respectively [2, 3]) can be prepared with dozens of SDAs [55], and at the same time (ii) they are the widest investigated AlPOs. Even $AlPO_4$-34 (CHA), which is other of the extensively studied aluminophosphates, mainly pushed by the catalytic interest in SAPO-34 in MTO process [32], can be prepared in the presence of different organic SDAs [174]. These three AlPOs practically cover all micropore range: small- (CHA), medium- (AEL) and large-pore (AFI) materials [2, 3].

The most evident example of such relationship between the straightforward synthesis and the selected topologies for being investigated is probably found in the comparison between the large-pore structures AFI ($AlPO_4$-5) and ATS ($AlPO_4$-36). Both have quite similar topologies with 1D pore system and very similar pore 12R apertures, so they have the same potential applications. Even both phases become competitive in the scarce crystallization systems in which ATS can be synthesized [175-177]. Moreover, the metal ion incorporation within the $AlPO_4$ frameworks, which gives them their primary potential applications, is almost compulsory for ATS-structured materials to be formed but it is expendable and sometimes self-defeating for AFI ones. Moreover, when both materials were tested as catalysts under similar conditions in certain reactions, MeAPO-36 materials often beat MeAPO-5 ones [37, 178 179]. In spite of that, the latter has received much more attention by scientific community, undoubtedly due to the straightforward and versatile methodologies reported.

Contrasting with such SDA versatility in the $AlPO_4$-5 materials preparation, practically any of the reported amines have very narrow synthesis conditions under which pure AFI-structured materials are crystallized. That low specificity is generally accentuated in the presence of doping metal ions. Therefore, it is a great challenge to find a highly specific SDA for this structure. By applying the above simple method, amongst the commercial amines, N-methyldicyclohexylamine (MCHA) was the one that best fits within the AFI pores (Figure 17). Confirming that perspective and the validity of the approach, MCHA was indeed shown as an extraordinary structure-directing agent for $AlPO_4$-5 materials and their Me-doped counterparts under a wide range of gel compositions and synthesis conditions, much wider than that given

Commented [ms21]: **Joaquín commented:** The relationship between the need of having metal ions for the crystallization of MeAPO-36 and the fact that they "beat" MeAPO-5 in a given catalytic reaction is not clear. Moreover, MeAPO-36 could eventually behave better than MeAPO-5 for some specific reaction, but this could not be generalized to other reactions. Please reconsider this whole paragraph.

Answer: We basically agree with the editor. It is true that in all cases we know in which MeAPO-5 and MeAPO-36 catalysts have been compared in test reactions (no matters if the reaction requires Bronsted acid sites or redox sites) always MeAPO-36 has been more active that its counterpart MeAPO-5. Among these studies, it is also included one work by the editor and coworkers in which MeAPO-5 and MeAPO-36 were tested as catalysts in the isomerization of m-xylene (Machado et al. J Catal 205, 299 (2002)). MeAPO-36 resulted much more active than MeAPO-5. The only exception we have found was in the corresponding Ti-containing AlPOs. Magnesium-free TAPO-5 was slightly more active than magnesium-containing TAPO-36 in the conversion of cyclohexanol to cyclohexanone (Akolekar and Ryoo J. Chem. Soc., Faraday Trans., 1996, 92, 4617-4621) but the possible effect of magnesium, which surely provided certain (undesired) acidity, was not considered. TAPO-5 was also more active than TAPO-36 in the oxidation of cyclohexane, but the catalytic activity per Ti center was higher in the case of TAPO-36 (M.H. Zahedi-Niaki et al. J Catal 177, 231 (1998)).

Nevertheless, we assume that we cannot generalize to all possible catalytic studies, so we have indicated that MeAPO-36 is more active that MeAPO-5 in certain reactions. And we have avoided to relate the higher activity of MeAPO-36 vs MeAPO-5 in those reactions with the role of heteroatom ions in the crystallization of these materials.

by any other amine reported up to then [84]. The MCHA specificity for the phase AFI was so high that further simulation studies were carried out trying to find extra explanation. These studies found so high specificity was also favoured by the impossibility of fitting MCHA in any of their possible stable conformation within the cavity of $AlPO_4$-34 structure (CHA) (Figure 17c), which is by far the most common phase co-crystallizing with $AlPO_4$-based AFI materials templated by so many amines or quaternary ammonia. In fact, the microporous $AlPO_4$-based phase that appears as an impurity of $AlPO_4$-5/MeAPO-5 phase in the MCHA system, especially when high loadings of heteroatom ions are present in the gel, is the large-pore $AlPO_4$-36/MeAPO-36, in whose pores MCHA molecules also fit well.

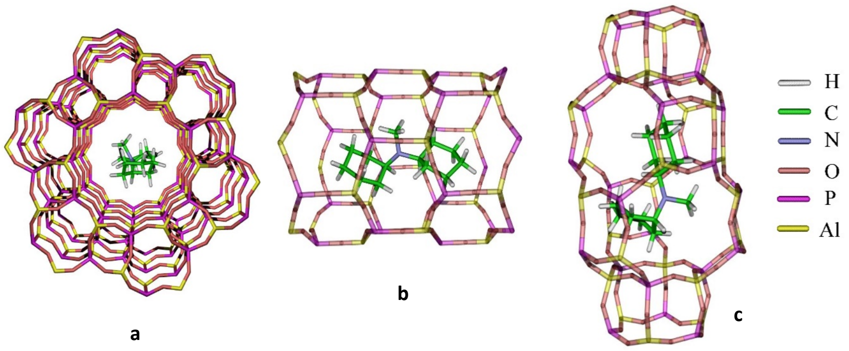

Figure 17. Energy minimised conformation of N-methyldicyclohexylamine within an $AlPO_4$-5 pore (*a* and *b*) and $AlPO_4$-34 cavity (c). (a) and (b) represent two different views of the one-dimensional channel showing the collinear alignment of the organic template molecule with the channel direction. Reprinted by permission from Springer Nature: Springer, Catalysis Letters, 'The Extremely High Specificity of N-Methyldicyclohexylamine for the Production of the Large-Pore Microporous AFI Material', M. Sanchez-Sanchez et al., Copyright 2003. [84

Commented [ms22]: **Joaquín commented:** This reference is probably wrong.

Answer: It is indeed wrong. Thanks. It has been corrected.

MCHA-templated $AlPO_4$-5 system is probably the system able to produce a pure $AlPO_4$ phase under the widest range of conditions and/or compositions ever reported. The specificity to AFI materials is much higher than triethylamine (TEA), triethylmethylammonium hydroxide (TEAOH) [84] or tripropylamine [180, 181], which are three of the most frequently used SDA for $AlPO_4$-5/MeAPO-5 materials. As an example of the phase specificity over so wide conditions, Co-doped $AlPO_4$-5 materials can be crystallized I pure form in the presence of MCHA under wide range of: (i) Me content (Me/(Me+Al) ratios from 0 to 0.15); (ii) pH of the starting gel (4 units!, from 5 to 9); or (iii) crystallization temperature (from 150 ºC to 200 ºC). Moreover, these materials can be fully synthesized in short crystallization times (in 3 hours), with excellent yields [84], are composed by relatively small crystal size and even contains some intercrystalline mesoporosity [180, 181].

Taking advantage of the exceptional properties of MCHA as a specific structure-directing agent, in the following subsections this amine is taking as a driven force of a 'travel' along the (catalytic) possibilities of metal-substituted AlPOs through the incorporation of very different metal ions (including some heavy metals), in different environments, in different oxidation states, through the co-incorporation of different heteroatoms, through diverse strategies to reduce the diffusional problems by either reducing the crystal size or introducing inter- and inter-crystalline, or through the catalytic performance of these microporous materials in different organic reactions.

b. Catalytic significance of structure-directing power of MCHA: SAPO-5 prepared at different pHs

The catalytic value of such specificity was initially made clear in the Pt-impregnated Si-doped $AlPO_4$-5 (the so-called Pt/SAPO-5) in the isomerization of n-heptane [182]. SAPO-5 materials resulted the only crystallized phase irrespective of any of the three Si sources (fumed silica, tetraethylorthosilicate or stabilized colloidal silica suspension in deionised water), in a large Si content range (Si/(Si+Al) ratio from 0 to 0.4) and, more importantly, in a large interval of pH (from 5 to 9). The samples prepared at pH 9 became much more acid that their counterparts prepared at pH 5, as made clear by pyridine temperature-programmed desorption studies (Figure 18A). Accordingly, the catalytic performance of the corresponding Pt-impregnated SAPO-5-pH-9 was several times higher than their homologous Pt/SAPO-5-pH-5 (Figure 18B). To the best of our knowledge, so large difference in catalytic activity of this kind of samples by just changing a synthesis parameter is unique, and it could not have been achieved in any other system than that templated by MCHA.

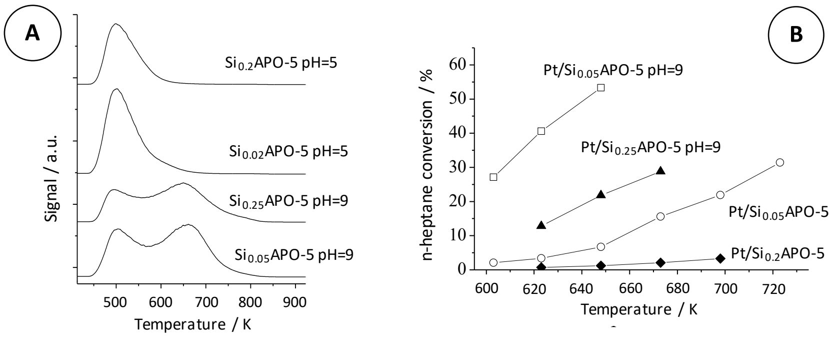

Figure 18. (A) Temperature-programmed desorption curves of pyridine (a) of SAPO-5 samples prepared with MCHA as SDA by systematically changed Si content and pH of synthesis gel. (B) Conversion of n-heptane in the isomerization reaction catalysed by the same SAPO-5 samples after impregnation of Pt. Adapted from Microporous Mesoporous Mater, 99, R. Roldan et al., Influence of pH and Si content on Si incorporation in SAPO-

5 and their catalytic activity for isomerisation of n-heptane over Pt loaded catalysts, 288-298, Copyright 2006, with permission from Elsevier [182].

It must be highlighted that $AlPO_4$-5/SAPO-5 materials have been also prepared under very different pH values of the starting gel (pH from 3 to 10) using triethylamine (TEA) as SDA [183]. The strategy was to use fixed and large amount of TEA (TEA/P ratio of 1.75) and controlled the pH by addition of different acids such as sulphuric, hydrochloric, acetic, nitric and hydrofluoric acids, also at high content. The study focused on kinetics of crystallization and on the changes in physicochemical properties of the resultant SAPO-5, particularly on crystal morphology. Unfortunately, all samples were composed by crystals of several micrometres, the different acidity of the samples were not discussed and no catalytic studies were carried out to prove any possible influence of pH synthesis in the catalytic performance.

c. Heteroatom versatility in MeAPO-5 prepared with MCHA

Although strictly speaking Si should not be among the heteroatom ions addressed in this Chapter, the preceding example emphasizes the importance of discovering more specific SDA in the synthesis of AlPOs as well as the power of MeAPO-5/MCHA system for academic and applied catalytic investigations in a systematic way. Obviously, such specificity has been extended to the incorporation of heteroatom ions more related to the subject of this chapter. Pure $AlPO_4$-5 and eleven heteroatom-substituted $AlPO_4$-5 were synthesized under exactly the same synthesis conditions and composition, excepting the nature of Me [180]. Although the metal ion nature played an important role in different physicochemical properties of the achieved samples such as crystal size, morphology arrangement of the crystals, intercrystalline mesoporosity, etc. (see below), MCHA invariably led to pure AFI-structured MeAPO materials [180].

d. Additional mesoporogen role of MCHA

In a catalytic context, the reactants accessibility to the active centres as well as the diffusion of products from the microporous catalysts to the reaction media could become as important as the intrinsic activity of the (metal) sites. In other words, the catalytic potential given by microporosity to the zeolitic materials through both size discriminating and reactants confinement, entails at the same time severe diffusion problems of molecules toward/from the pores, lowering both the conversion and the catalyst lifetime by blocking the pores. That is why the avoiding/reducing of diffusion problems is being paid so much attention, and different synthesis or post-synthesis strategies have been developed [184]. Among these approaches, the synthesis of nanocrystalline samples and the introduction of either inter- or intracrystalline mesoporosity are the most direct ones, and consequently they have been the most broadly explored. The diffusion of reactants/products is even more limiting for structures with unidirectional pore systems, such as the case of $AlPO_4$-5 and many other microporous crystalline aluminophosphates, which besides used to be formed by very large crystals. In this sense, it can be highlighted that the direct preparation procedure of Me-substituted $AlPO_4$-5 in the presence of MCHA with no synthesis/post-synthesis effort/modification, already gives MeAPO-5 materials of nanocrystals orderly agglomerated/aggregated in micron-sized particles (Figure 19A). For comparison purposes, crystals of a CoAPO-5 prepared with TPA as SDA is also shown in Figure 19A. The crystals of CoAPO-5 prepared with MCHA are ca. 3 order of magnitude smaller! Moreover, the ordered aggregation of the nanocrystals in the particles leads to the existence of intercrystalline mesoporosity, suggested by SEM images (Figure 19A) and confirmed by N_2 adsorption/desorption isotherms (Figure 19B). The ability of MCHA to direct AFI-structured $AlPO_4$-based materials with so small crystal size suggests a strong structure directing effect towards such topology, as the achievement of nanocrystals implies ease, simultaneous and abundant nucleation in very different parts of the synthesis gel. Such idea is also supported by the rapid crystallization of these materials in the presence of MCHA: at crystallization temperature of 175 ºC, (i) in conventional Teflon-lined autoclaves, a full crystallized CoAPO-5 can be achieved in just three hours [84]; in a synchrotron cell, where the kinetics of heating is higher, XRD diffraction peaks appeared after crystallization times as short as 66 minutes [99]; under microwave-assisted heating, CoAPO-5 is full-crystallized after 1 hour [181].

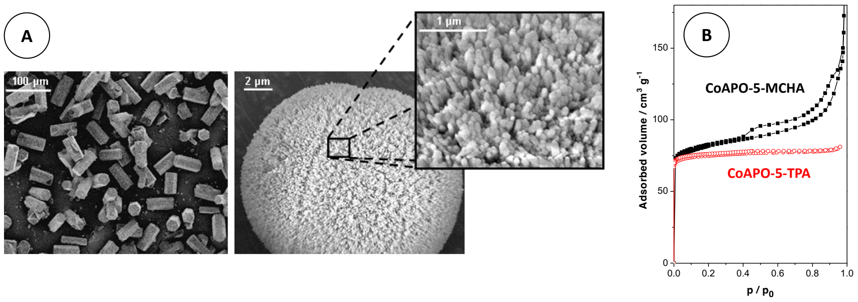

Figure 19. (A) SEM images of the samples CoAPO-5 prepared with TPA (left) and MCHA (right) as SDAs. An insert of a portion of a CoAPO-5-MCHA particle is also shown. Note through the size-scaled bar the very different magnification used for the shown images, what gives an idea of the difference in particle/crystal size. (B) N_2 adsorption/desorption isotherms at -196 ºC of the same samples (CoAPO-5-TPA in red and CoAPO-5-MCHA in black). Adapted from Catalysis Today, 179, A. Manjon-Sanz et al., Towards the control of intercrystalline

mesoporosity in inorganic microporous materials: The case of CoAPO-5, 102-114, Copyright 2011, with permission from Elsevier [181].

Interestingly, each heteroatom ion strongly conditioned the morphology and crystal size, and consequently the shape, the consistence or the intercrystalline mesoporosity of the arranged particles of the resultant MeAPO-5 crystallized from the MCHA-containing gel, even for low dopant loadings (Me/P ratio of 0.04) [180]. Figure 20 shows the SEM images and the isotherms of different as-prepared MeAPO-5/MCHA samples. It must be highlighted that the MeAPO-5 samples are not calcined, so the shown porosity is exclusively due to the intercrystalline mesoporosity. The MeAPO-5 samples doped with Zr, Cr, Si, Fe or the non-doped $AlPO_4$-5 have similar crystal size and arrangements than these shown for Sn(II)APO-5, the MeAPO-5 samples where Me is either Mg or Mn are morphologically similar to the CoAPO-5 samples, whereas the morphology of any of the samples doped with Zn, V or Sn(IV) are unique in this series.

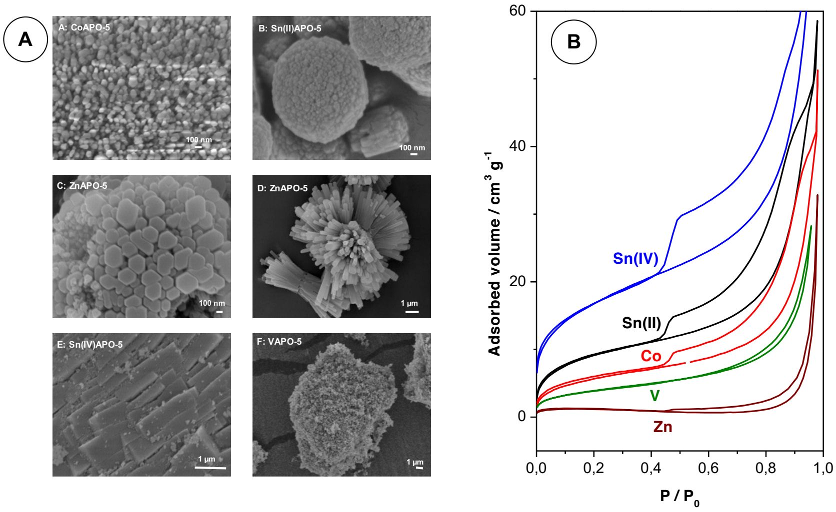

Figure 20. SEM images (A) and N_2 adsorption/desorption isotherms at 77 K (B) of as-synthesized Co-, Sn(II)-, Zn-, Sn(IV) and V-doped $AlPO_4$-5 samples prepared with MCHA as SDA. Adapted from Microporous and Mesoporous Materials, 131, A. Manjon-Sanz et al., Non-templated intercrystalline mesoporosity in heteroatom-doped AlPO4-5 using N-methyldicyclohexylamine as structure-directing agent, 331-341, Copyright 2010, with permission from Elsevier [180].

Although the influence of the heteroatom ion nature seems to be fundamental in both the crystal size and intercrystalline mesoporosity of the MeAPO-5 prepared with MCHA, it must be remembered that so many synthesis parameters can be varied along a considerably large range without changing the nature of the crystallized phase, taking advantage of the high specificity of MCHA towards the AFI materials. Moreover, it precisely offers a unique opportunity of studying the effect of these parameters in the morphologic and textural properties of an $AlPO_4$/MeAPO material. In this sense, a wide and systematic study with CoAPO-5/MCHA system was carried out [181]. The magnitude and the homogeneity of intercrystalline mesoporosity of CoAPO-5 samples were improved at short crystallization times (2 h), at the highest tested crystallization temperature (210 ºC), at the high Co content (Co/P ratio of 0.08), at low pH of the starting gels (pH 5), and at high dilution (H_2O/P ratio of 25), the two latter being the most influent parameters. However, overcoming any other influence, the microwave-assisted heating led to a decrease and a homogenization of crystal width and generated more ordered mesoporosity of smaller pores (Figure 21).

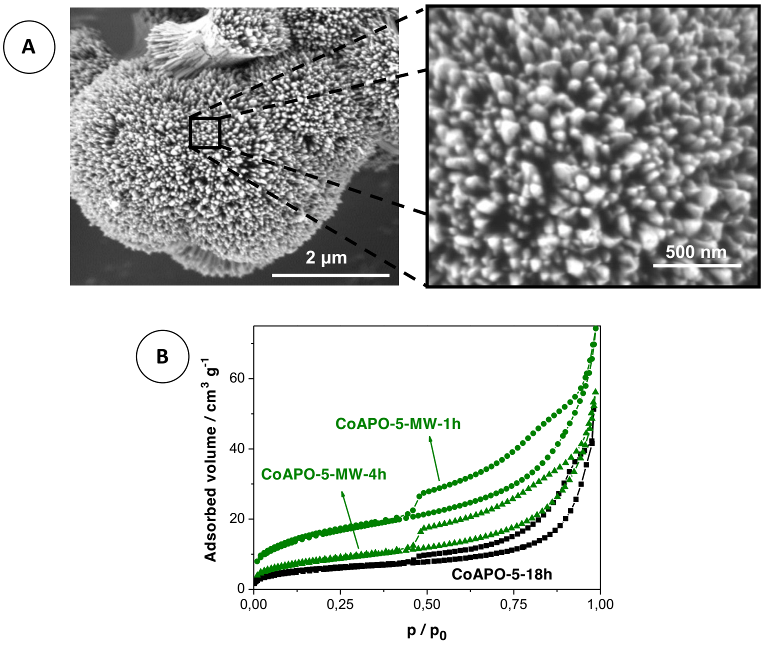

Figure 21. SEM images (A) and N_2 adsorption/desorption isotherms at 77 K (B) of microwaved-assisted as-synthesized CoAPO-5 sample prepared with MCHA as SDA for 1h and 4h, respectively (green curves). For comparison purposes, the isotherm of CoAPO-5 prepared with the same SDA but under conventional heating for 18 h is also shown (black curve) in (B). Adapted from Catalysis Today, 179, A. Manjon-Sanz et al., Towards the control of intercrystalline mesoporosity in inorganic microporous materials: The case of CoAPO-5, 102-114, Copyright 2011, with permission from Elsevier [181].

e. Generating intracrystalline mesoporosity in the MCHA-MeAPO-5 system

The generation of the intercrystalline mesoporosity in certain AlPOs, particularly in these having an 1D pore systems, does not always imply a substantial improvement of the diffusional problems, because their crystals used to be of a rod-like morphology in such a way that the intercrystalline mesoporosity between such crystals does not communicate the microporous of different crystals located within the same particle. Two further strategies have been developed to enhance the chemical (reactants and products) diffusion: (i) the introduction of intracrystalline mesoporosity and (ii) the change of morphology making that the 1D pores run along the short dimension of the crystals [185, 186]. The former is relatively common in zeolites by either the post-synthesis treatments of the framework by reagents able to partially dissolve silica, such as NaOH, NH_4OH, HF, etc., or by the inclusion of different macromolecules or nanoparticles during the synthesis processes, which subsequently act as mesoporogens (generators of mesopores) once they are removed by calcination [183]. To the best of our knowledge, the post-synthesis strategy has not been successful in $AlPO_4$-based materials, probably due to the difficulty of finding a solvent able to efficiently generate mesoporosity in the $AlPO_4$ crystals keeping their topology. The second strategy has been applied with relative success to different $AlPO_4$, such as SAPO-34 materials [187, 188], but the afforded mesoporosity is however far from that generated in zeolites.

Commented [ms23]: **Joaquín commented:** What do you mean by weak solvent?

Answer: Now we think that the adjective weak was not appropriately selected for this sentence. We have removed it and we have modified a bit the sentence in order to clarify what we meant.

One of the most celebrated approaches to reduce diffusional problems in zeolites is the crystallization of the framework inside of a mesoporous amorphous commercial carbon matrix, which in this case is not a mesoporogen but provides confinement space allowing the nucleation of the zeolitic crystals but severely limiting the crystal growing further to the available pore dimension of the carbon [189, 190]. In other words, it was a method to reach nanocrystalline zeolites. In spite of the success of this method in the synthesis of nanocrystalline zeolites, it was not applied to AlPOs/MeAPOs systems during years, probably because the method requires starting from soluble sources, which is not common in synthesis of AlPOs and not easy to be implemented in so phase-unspecific systems. In this context, MCHA is a quite phase-specific system towards $AlPO_4$-5/MeAPO-5 materials, and it easily directs the crystallization of these materials by changing conventional sources of Al, which are almost always insoluble solid, by the highly soluble-in-water source $AlCl_3 \cdot 6H_2O$ [191]. After that previous optimization, the reactants necessary to form CoAPO-5 were incorporated within the carbon matrix one by one through successive witness impregnation. The subsequent hydrothermal treatment generated CoAPO-5/Carbon composites (Figure 22). The size of the pencil-like CoAPO-5 crystals were of several micrometers, indicating that the resultant CoAPO-5 material was not nanocrystalline, as intended. Paradoxically, the peaks of the XRD pattern were quite broad indicating the expected nanocrystalline nature (Figure 22). This apparent incongruity was solved out through the calcination of the sample (Figure 23). The apparently solid pencil-like crystals of CoAPO-5 actually contained extensive amount of embedded carbon matrix, which are burned during the calcination, leaving substantial both inter- and, more important, intracrystalline mesoporosity.

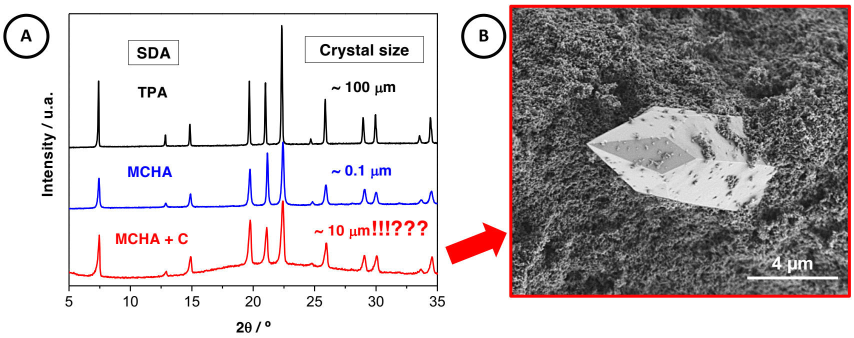

Figure 22. (A) XRD patterns of three as-prepared CoAPO-5 samples prepared with TPA (top, black line), MCHA (middle, blue line) and MCHA within porous carbon BP-2000 (bottom, red line). (B) SEM image of the latter showing a pencil-like crystal emerging from the host carbon matrix. Adapted with permission from [191]. Copyright 2017 American Chemical Society.

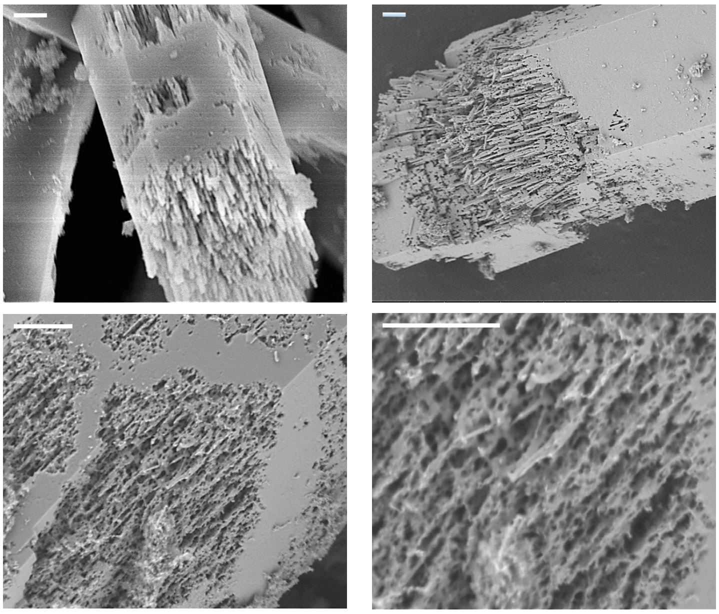

Figure 23. SEM images of different particles forming the sample CoAPO-5 shown in Figure 22 after calcination. The scale bar indicates 1 µm in all cases. Adapted with permission from [191]. Copyright 2017 American Chemical Society.

f. Incorporation of Me in different oxidation states in MCHA-MeAPO-5 system: Sn and Ti

The high specificity of MCHA towards AFI-structured $AlPO_4$-based materials has been also used in the incorporation of ‘uncommon’ heteroatom ions. It is particularly interesting the incorporation of a given heteroatom in different oxidation states. In that way, the same heteroatom could potentially reach different environments in the $AlPO_4$ framework. That environment versatility is not possible to be designed in zeolites, as Si^{4+} is the only ion to be substituted by the incorporated heteroatoms.

The first study in this sense was carried out with the incorporation of tin. As a promising antecedent, Sn-beta was shown to be an excellent Lewis catalyst in different reactions such as Baeyer-Villiger [8, 192] or Meerwein-Ponndorf-Verley [193] ones. Meanwhile, the reported SnAPO materials before the irruption of MCHA had very scarce impact. All these SnAPOs had been prepared from Sn(IV) sources, whose incorporation mechanism is potentially varied and of doubtful effectiveness in terms of acidify if 2 Sn(IV) atoms substitutes a pair Al(III)-P(V). However, it is well-known that tin has two quite stable oxidation states, 4+ and 2+. The incorporation of Sn(II) in an $AlPO_4$-5 framework has necessarily to be in Al positions, and no Sn-O-Sn environments should be formed. Therefore, all Sn(II) centres should be equal and each incorporated Sn(II), unlike Sn(IV), entails the generation of a Brönsted acid site. Such predictions were indeed confirmed once both materials Sn(IV)APO-5 and Sn(II)APO-5 were successfully prepared taking advantage of the high specificity of MCHA [194]. The characterization by means X-ray diffraction (through their unit cell parameters) UV-visible spectroscopy, solid-state ^{31}P MAS NMR and Temperature-Programmed Desorption (TPD) of ammonia, confirmed that all Sn(II) but just a part of Sn(IV) were rightly incorporated into the $AlPO_4$ framework in different environments and that the acidity of Sn(II)APO-5 was higher than that of Sn(IV)APO-5 (Figure 24). Confirming this characterization evidence, the catalytic performance of Sn(II)APO-5 in the Friedel-Crafts acylation of anisole, which requires the presence of Brönsted acid sites, clearly overcomes that given by Sn(IV)APO-5, SAPO-5 and even by a zeolite H-Al-beta [194].

Commented [ms24]: **Joaquín commented:** I think this number does not correspond to the reference you wanted to cite here.

Answer: It has been renumbered.

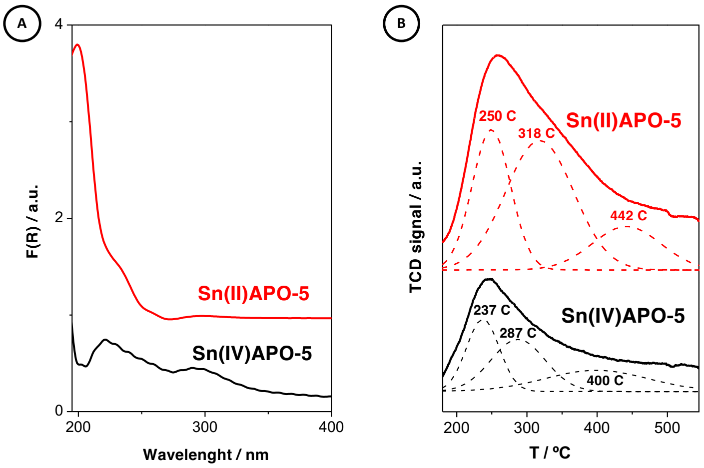

Figure 24. DR-UV-vis spectra (A) and NH_3-TPD profiles (B) of Sn(IV)APO-5 (red lines) and Sn(II)APO-5 (black lines) samples. In Fig. 24B, the three components in which each profile has been decomposed are also shown to underline the higher acidity of the Sn(II)APO-5 sample. Reproduced from ref. [194] with permission of The Royal Society of Chemistry.

The incorporation of Ti into zeolite frameworks revolutionized the applications of inorganic microporous materials, as they started being used as catalysts in so many Fine Chemistry reactions [195, 196]. It was the germ of the metal-zeolites, the subject of this issue. Ti-zeolites have been the most extensively investigated metal-zeolites, not only because of their pioneer condition but also because of their outstanding catalytic performance in different reactions of industrial interest. On the contrary, Ti-containing AlPOs, which are known as TiAPO, TiAPOs or TiAlPOs, have been scarcely studied, undoubtedly due to their much more modest catalytic power compared with their counterpart Ti-zeolites. In principle, there are several reasons behind that substantial difference. Firstly, $AlPO_4$ framework is quite hydrophilic (Table 1) contrasting with the hydrophobic nature of the Al-free zeolites, which severely limits the application of the former in organic reactions. Secondly, the incorporation mechanism of heteroatom ions into microporous materials, which is richer in AlPOs than in zeolites (Table 1), could become somehow unfavourable in aluminophosphates when tetravalent ions are desired to be incorporated. It is due to: (i) its isolated incorporation (by either Al or P) necessarily entails a charge deficiency/excess, so their intrinsic activity is seriously modified, particularly by the existence of Brönsted acid sites Ti-OH-Al if the most accepted Ti incorporation in P sites of an $AlPO_4$ framework is assumed; and (ii) the incorporation mechanism is not unique but several mechanisms and even a combination of them can be taken place in a given material, and then several types of active sites could be found. Finally, the intrinsic activity of Ti in an $Ti(OSi)_4$ environments is much more active than in an $Ti(OAl)_4$ environments. These three facts (hydrophilicity, associated Brönsted acidity and intrinsic activity) are indeed responsible of the much lower activity of Ti-Al-zeolites than that of Al-free Ti-zeolites [197, 198], and it is expected that their negative influence is higher in the catalytic activity of TAPOs.

Until recently, all the TAPO materials had been synthesised starting from Ti(IV) sources. However, since 2013, again taking advantage of the high specificity of MCHA towards AFI-structured materials, the synthesis of TAPO-5 using Ti(III) source was proposed and carrying out the gel formation and crystallization under inert conditions, in order to avoid the spontaneous oxidation of Ti(III) to Ti(IV) under oxidant atmosphere [106, 199-202]. This approach could in principle solve two of the three above-mentioned drawbacks of TAPOs vs Ti-zeolites: (i) the Ti environment would be $Ti(OP)_4$ instead of $Ti(OAl)_4$ found in conventional TAPOs, and (ii) the Brönsted acidity associated to Ti incorporation is avoided. The third drawback, i.e. the hydrophilic nature, is basically unaffected. Once Ti(III)APO-5 material was exposed to the ambient atmosphere, it was transformed to a Ti(IV)APO-5, which however possesses very different physicochemical properties (as evidenced by means of thermogravimetric analysis and UV-visible and multinuclear solid-state NMR) to the conventional TAPO-5 (Figure 25). These new TAPO-5 materials were catalytically tested in the oxidation of cyclohexene with anhydrous H_2O_2, leading to two important conclusions: (i) they can reach catalytic conversion quite similar to Ti-beta, a large-pore Ti-containing zeolite having a 3-D pore system [199], and (ii) not least, unlike the epoxidation route followed by the oxidation of cyclohexene by peroxides in the presence of Ti-zeolites, this new TAPO-5 catalysed the allylic oxidation of the olefin under the same conditions [199, 200, 202]. In other words, TAPO-5 materials prepared with Ti(III) sources could become as active as Ti-zeolites under certain experimental conditions and both materials could be catalytically complementary rather than competitors.

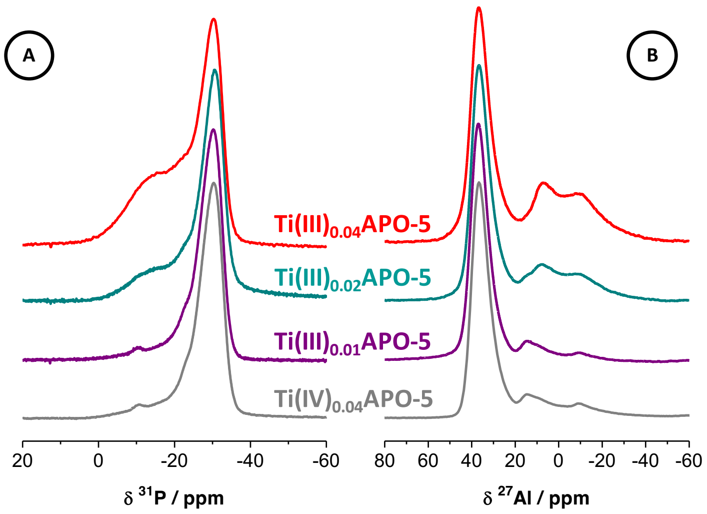

Figure 25. ^{31}P (A) and ^{27}Al (B) MAS NMR spectra of a series of Ti(III)APO-5 samples with different Ti content. The spectra of a Ti(IV)APO-5 having the same Ti content than the Ti-richest Ti(III)APO-5 sample is also shown for comparison purposes. Adapted from Microporous Mesoporous Mater, 190, A. Alfayate et al., Incorporation of Ti(III) into the $AlPO_4$-5 framework by direct synthesis, 334-345, Copyright 2007, with permission from Elsevier [106].

To the best of our knowledge, this is the first time that a heteroatom in an unstable oxidation state has been incorporated into an $AlPO_4$ framework. Moreover, this strategy has been rationally designed to change the metal environment within the microporous framework and then their catalytic behaviour.

g. Multi-metal-substituted $AlPO_4$-5 materials: synergic catalytic effect

The simultaneous incorporation of different heteroatom ions in zeolites [203-205] and AlPOs [206-208], each one to generate centres of different nature (the most common being redox and acid centres or Brönsted and Lewis sites), is well known and has been rationally designed to catalyse successive steps of a given reaction in just one step. However, the synergic catalytic effect of two different metal ions incorporated in microporous materials providing the same catalytic functionality (for instance, two redox catalytic centres), which is relatively common in metal-supported oxide-based catalysts, does not seem easy to be reached in metal-substituted crystalline microporous materials. The conventional synergic effect is based on the modification of the electronic properties (and then the catalytic potential) of an active metal by a second supported/incorporated metal, in such a way that the resultant multi-metallic catalysts become more active/selective than the corresponding monometallic counterparts. In zeolites and zeotypes, the isomorphic incorporation of metal ions generally leads to isolated metal sites surrounded by oxygen atoms and subsequently by the framework tetrahedral atoms (Si in the case of zeolites, P and/or Al in AlPOs) in the second coordination sphere. Therefore, the electronic influence of a second metal ion (incorporated in poor loadings imposed by zeolite/zeotype limitation) over the active metal is quite unlikely.

Nevertheless, simulation studies on the complex mechanism of the oxidation of hydrocarbons by oxygen in Mn- and Fe-substituted AlPOs [147-155] indicates that each transition metal can favour a particular step of the global mechanism. In particular, it was expected that co-doped FeMnAPO samples are more active than their counterpart FeAPO and MnAPO samples for a given metal content [153]. That prediction was indeed experimentally corroborated [209]. Therefore, a synergic catalytic effect is also possible to be reached in multi-metal-substituted $AlPO_4$ materials. However, this synergic effect is conceptually different to that frequently used: the co-incorporation of metal ions does not modify the electronic properties with respect to these of the same metals individually incorporated in the same $AlPO_4$ structure, but any metal could act effectively in different steps of a given reaction, accelerating the global kinetics.

MCHA/$AlPO_4$-5 system was again the option selected by Raja et al. for a systematic study on the multi-metal-substituted $AlPO_4$-based catalysts [210, 211]. Pure AFI materials were crystallized irrespective of the number and/or loading of dopants. Metal ions as heavy as Ru(III) were used and the simultaneous incorporation up to three different metals (in the sample RuZnSnAPO-5) was achieved [210]. Figure 26 shows the catalytic benefits of using bimetallic MeAPO-5 catalysts against their monometallic counterpart in the oxidation of cyclohexene using acetylperoxyborate as the oxidant. The improvement of the turnover of co-doping $AlPO_4$-5 with both Co and Ti in the oxidation of cyclohexene becomes ca. four times with respect to CoAPO-5 and twice with respect to the monometallic TAPO-5. In the heavy metal containing RuSnAPO-5 samples, the catalytic enhancement, although evident, is not as high as in the previous example, because the monometallic SnAPO-5 and RuAPO-5 are already quite active.

In a similar way, the bimetallic Ti,V-doped $AlPO_4$-5 was also more active than their monometallic homologues in the same reaction [211]. Its characterization by means a combination of HYSCORE EPR and in situ FTIR studies, indicated that V and Ti centres play distinct roles in a concerted fashion that synergistically boost the overall catalytic performance. Ti centres link the oxidant to activate it through the formation of peroxo species, whereas V possesses lower barrier than Ti to carry out the oxidation itself once the oxidant is activated [211].

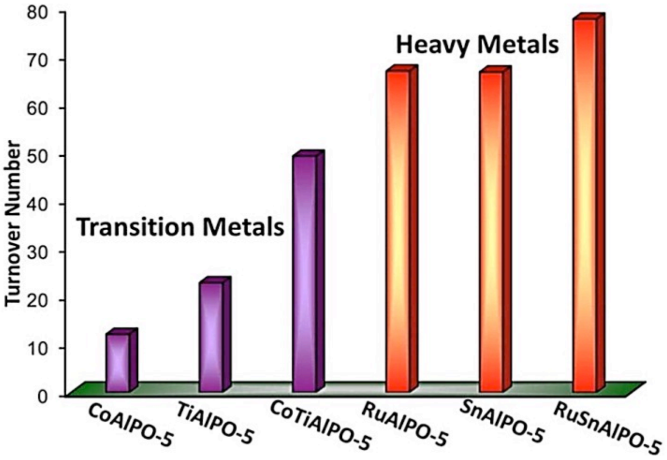

Figure 26. Turnover number of the different doped $AlPO_4$-5 materials prepared with MCHA as SDA in the epoxidation of cyclohexene with acetylperoxyborate at 66 ºC. The turnover of the samples doped with transition metals (Co and/or Ti) are plotted as purple columns, and the samples doped with heavy metals (Ru and/or Sn) are given as orange columns. Reprinted with permission from [210]. Copyright 2012 American Chemical Society. Further permissions related to the material excerpted should be directed to the ACS.

.

5.2. Designing new SDAs for AlPOs/MeAPOs able to be prepared by just one SDA

If the low phase-specificity is problematic and quite limiting for AlPO materials that can be non-specifically prepared with dozens of known SDAs, it becomes much more serious when only one (low phase specific) SDA has been described for a given $AlPO_4$ structure. Obviously, the knowledge of a unique SDA able to direct the crystallization of a given structure does not imply high specificity. Also in these cases, the above described strategy to find new amine-based SDA for a particular 1D-pore $AlPO_4$ topology can be an elegant and simple solution. In this section, the application of that approach is described for two additional $AlPO_4$ structures: the large-pore ATS ($AlPO_4$-36) and the small pore ATN ($AlPO_4$-39) [171]. Before this approach was applied to these systems, the only described SDA able to direct the crystallization of these materials were tripropylamine and dipropylamine (DPA), respectively. The first one can also lead to AFI-structured materials, whereas DPA is probably the less phase-specific amine as it has been used for at least 10 different $AlPO_4$-based materials (ATN, AFO, AEL, VFI, ATO, APC, AFS, GIS, AFS or AFY) [131-133]. In addition, DPA mainly tends to give $AlPO_4$-11 and the experimental conditions to generate $AlPO_4$-39/MAPO-39 are really narrow [57].

Figure 27 shows the fits of the conventional SDAs for AlPO$_4$-5, -36 and -39, as well as the fits of the new proposed SDAs for these structures. Both conventional and proposed SDAs are configured as the model predicts, that is, in its most stable conformation and with the bulkiest R hydrocarbon substituent group in the amine NR$_3$ running along the AlPO$_4$ channel [171]. Given the high symmetry of both DPA and ATN pore, the fit is relatively good from the shape point of view but it is quite improvable in terms of size. Diisobutylamine (DiBA) is not as symmetric as DPA, but in that conformation the general fit within the ATN pore could be better than that given by DPA. The experiments confirmed that DiBA was at least as specific as DPA in the preparation of CoAPO-39 [171]. Like DPA, when some experimental conditions were altered, CoAPO-11 (AEL topology) appeared as impurity, and even it could be purely crystallized with DiBA. At least, an alternative to the unique SDA able to lead ATN topology was found.

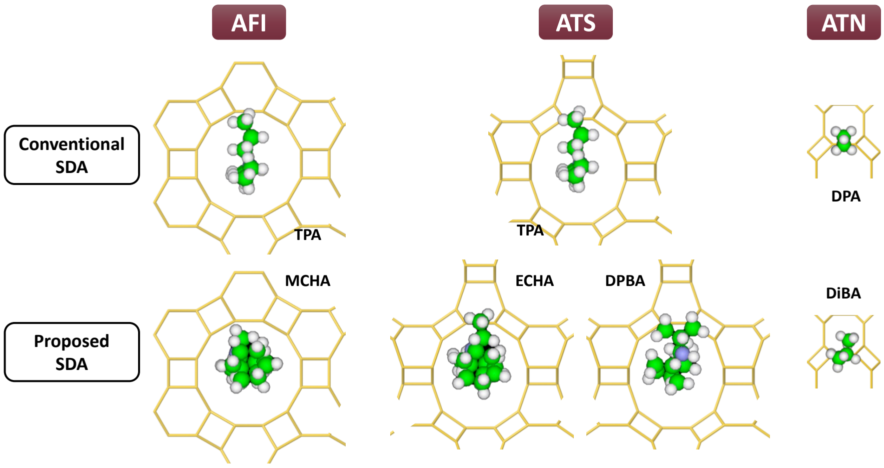

Figure 27. Schematic representation of some conventional (top) and proposed (bottom) amine-based SDA fitted within the pores of the 1D topologies AFI (left), ATS (middle) and ATN (right).

In the case of ATS-structured MeAPO materials, the fit of TPA within their pores was rather poor but a bit better than in AFI pore (Figure 27). Tripropylamine (TPA) has been selected as the SDA for AFI among the dozens of SDAs able to crystallize AlPO$_4$-5 materials [56] precisely to compare its fitting to that found in ATS structure. The slightly better fit in ATS than in AFI pores could be behind the fact that TPA was the only known organic SDA that led to the formation of ATS before applied our simple method. The relatively poor fit of TPA within ATS pore suggested the existence of a great room in the search of new SDAs for such topology. In principle, much better fit was achieved by the commercial amines N-ethyldicyclohexylamine (ECHA) and diisopropylisobuthylamine (DPBA) (Figure 27) [171].

Indeed, these two new templates were experimentally able to direct the crystallization of ATS-structure $AlPO_4$-based materials in an efficient way.

An exhaustive study of the crystallization kinetics of CoAPO-36 together with some simulation calculations were also carried with the three amine-based SDAs. It confirmed that the two new proposed SDA needed less activation energy to produce these materials (Figure 28) [212], which is consistent with the much quicker crystallization experimentally found for DPBA and ECHA. In addition, computational calculations confirmed that the interaction energy (defined as the difference between the total energy of the framework/template system and the energy of an isolated gas-phase template molecule) is much lower for DPBA and ECHA than for TPA. In spite of such comparison can be questioned as kinetically controlled rates of reaction are compared with the thermodynamic products of the energy minimization, previous studies shown an unequivocal and strong correlation between energetics of template fit with rates of crystallization for a series of zeolite structures, with the lower energy template fits resulting in increased rates of crystallization [213].

Therefore, the effectiveness in filling the pore, that is, the goodness of the fit SDA-pores shown in Figure 28 can be taken as a reliable indication of the power of an amine as structure-directing agent in AlPOs. In other words, we believe that the structure-directing effect of the amines in the synthesis of $AlPO_4$-based materials indeed includes an important contribution of 'template' effect, although some other contributions to the SDA role such as pH controller, compensation of the charge framework (if any) or the simple filling the confined space of the pores, etc., would call into question this fact. Such contribution of the 'template' effect to the general structure-directing role could become an important tool in the rational design of more efficient and more specific organic SDA for $AlPO_4$-based materials.

Commented [ms25]: **Joaquín commented:** It seems to me that a good pore filling is already an expression of a good interaction energy between the organic molecule and the framework, something that it is involved in the so called template effect.

Answer: We also agree with that.

In this paragraph what we tried is to emphasize that the generally low phase specificity attributed to the amines in the synthesis of AlPOs can be improved by simple models that takes into account the size and/or shape of the SDA within the pores of the desired structure. If the use of the term `
'template' has been relegated to the detriment of the use of SDA in zeolites because the number of examples in which the size/shape of the organic SDA well matches with the size/shape of the zeolitic pore, are really scarce, in the case of AlPOs, where the phase specificity is normally much lower, one can think that the role of amines as pH controller, charge compensating, etc. but rarely as a proper template. So many researchers have in mind that DPA can direct the synthesis of 10 different AlPO-based material or that AlPO4-5 can be prepared with more than 50 amines.
Proving that the SDAs can play certain but significant role as proper templates is an important fact promoting the rational design of more effective and phase-selective organic molecules as structure-directing agents of (metal-doped) AlPO-based materials.

In summary, along this section it has been made clear that finding specific and effective SDAs for the preparation of metal-substituted AlPOs could be key in two contexts: (i) in an academic one, allowing to carry out systematic works in which just one parameter (metal nature, synthesis pH, etc.) could be varied keeping practically constant the rest; (ii) in the context of application, improving the (catalytic) properties of a given MeAPO by different strategies such as reducing crystal size, introducing inter- or intracrystalline mesoporosity, controlling the chemical environment of the metal dopants by rational choice of their oxidation state (even if they are unstable under ambient conditions), incorporating very large heteroatom ions including heavy metals or favoring the synergic effect when more than one heteroatom are incorporated.

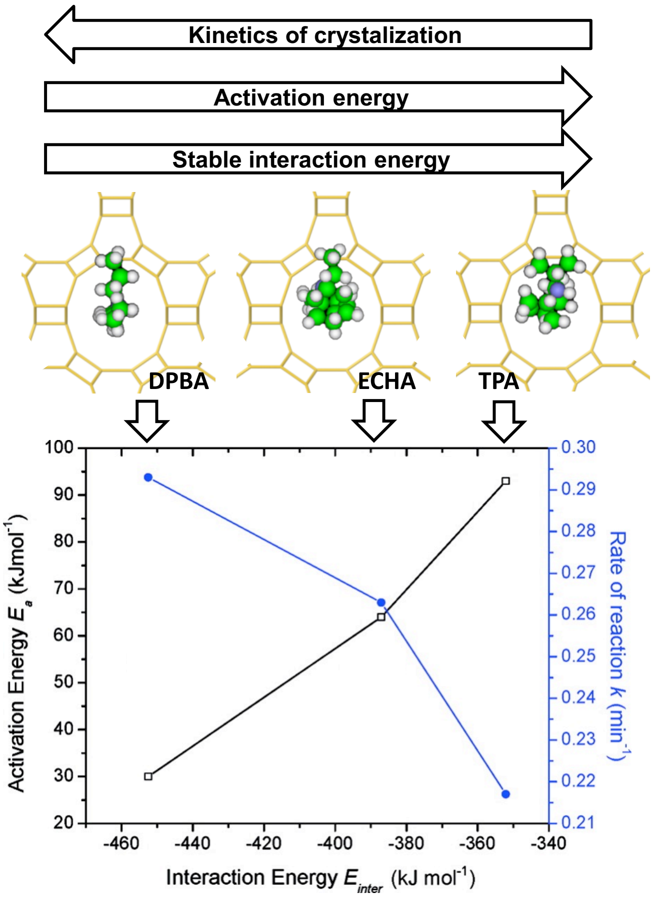

Figure 28. On the bottom, computational calculated interaction energies of the SDAs TPA (left), ECHA (middle) and DPBA (right) within an CoAPO ATS pore plotted versus both activation energy (black line, left Y-axis) and rate of crystallization (blue line, right Y-axis). Reprinted with permission from [212]. Copyright 2012 American Chemical Society. In the middle, representation of the fit of the three SDA within the ATS pore. On the top, order of kinetics of crystallization, activation energy and interaction energy for the three SDAs.

Commented [ms26]: **Joaquín commented:** I think there is a mistake in the plot, for in the plot the lowest activation energy corresponds to TPA, opposite to what it is written in the text. Please revised this.

Answer: There was indeed a mistake in the figure. Thanks for that. It has been corrected.

6. Conclusions

Aluminophosphate microporous materials (AlPOs) are the zeotypes possessing most similar properties to zeolites, especially in their use as catalysts. Thus, like zeolites, AlPOs are crystalline, microporous and thermally stable (depending on the structure and hetero-atom content) and can be crystallized in a variety of topologies (some of them can also be prepared as zeolite forms) having small, medium, large and/or very large micropores. Besides, both families of microporous materials have also in common the general use of amines and or quaternary ammonium hydroxides as structure-directing agents.

The general common properties with zeolites make $AlPO_4$-based materials being used in similar applications than zeolites. However, the real potential of $AlPO_4$-based materials is mostly found in the diversity of heteroatom incorporation by isomorphic substitution. Such diversity includes oxidation states, cation sizes, incorporation mechanism, pH of the incorporation or final chemical environment in the framework, which are difficult to achieve by silica-based zeolite frameworks. In addition, some microporous $AlPO_4$ topologies cannot be prepared with a SiO_2-based composition.

It must be noted that a range of divalent cations with catalytic relevance as Co^{2+}, Mn^{2+}, Fe^{2+}, etc. can be easily introduced into the $AlPO_4$ framework (in Al^{3+} sites) of these materials; similarly, tetravalent ions as Ti^{4+}, V^{4+} can be introduced in P^{5+} sites. Besides, the $AlPO_4$ frameworks allow these heteroatoms to change its oxidation state (normally in redox cycles 2+ to 3+) as many times as the reaction requires with no leaching. These catalysts have been successfully used in the highly-demanding oxidation of inert alkanes with air or oxygen as oxidants. The catalytic results combined with an adequate selection of advanced characterization techniques and computational calculations led to a deeper understanding of the active sites and the reaction mechanism. And such knowledge allowed the rational design of more active catalysts by careful choice of the metal nature as a function of their Me^{2+}/Me^{3+} ratio in the calcined catalysts. Similarly, the right choice of the Me content and the structure depending of the reactants to be catalyzed led to the design of regioselective catalysts.

Commented [ms27]: **Joaquín commented:** This is the first time leaching is mentioned. It would have been better to mention it in the main text, so please do it.

Sankar, I think it is better if you include in the main text a (couple of) mention about the absence of metal leaching, particularly in the Co2+/Co3+, Mn2+/Mn3+, Fe3+/Fe3+ systems, under the catalytic conditions.

Some of the apparently intrinsic disadvantages of $AlPO_4$-based materials can be solved out. That is the case of the low phase-specificity of amines as structure-directing agents, which limits both the systematic studies and the improvement of the physicochemical properties of the MeAPO catalysts. Starting from a simple method based on the most probable and stable conformation of the amines along the 1D-pore topologies, new SDAs was found for ATS and ATN structures as effective alternatives to the known SDAs for these materials. Moreover, MCHA showed to be most specific SDA for AFI materials. Taking advantage of that, all MeAPO-5 materials can be prepared under the same conditions by just changing the metal (Me) nature. In addition, it allows the control of parameters as metal content, metal ion size, incorporation of metals in different oxidation state, metal environment, crystal size, hierarchical meso-/micro-porosity, or easy/direct co-incorporation of different metal ions in a given $AlPO_4$-5 framework promoting synergic catalytic effects.

As a final and more general conclusion, metal-substituted aluminophosphates provide unique features to the exciting catalytic world of heteroatom-containing microporous materials.

Acknowledgments

GS thank EPSRC and Royal Society for funding. MSS acknowledges the financing by Spanish State Research Agency (AEI) and the European Regional Development Fund (FEDER) through the Project MAT2016-77496-R (AEI/FEDER, UE). Thanks to Dr. A. Alfayate for kindly providing us a figure.

7. References

[1] Cronstedt AF (1756) Kongl Vetenskaps Academiens Handlingar Stockholm 17:120-123.

[2] http://www.iza-structure.org/databases/.

[3] Baerlocher Ch, McCusker LB, Olson DH (2007) Atlas of Zeolite Framework Types (6th ed.), Elsevier, Amsterdam.

[4] Taramasso M, Perego G, Notari B (1983) US Patent 4 410 501

[5] Barrer RM, Freund E (1974) J Chem Soc Dalton Trans 10:1049-1060.

[6] Rigutto MS, van Bekkum H (1991) Appl Catal 68:L1-L7.

[7] Dongare MK, Singh P, Moghe PP, Ratnasamy P (1991) Zeolites 11:690-693.

[8] Corma A, Nemeth LT, Renz M, Valencia S (2001) Nature 412:423-425.

[9] Chu CT, Chang CD (1985) J Phys Chem 89:1569-1571.

[10] Calis G, Frenken P, de Boer E, Swolfs A, Hefni MA (1987) Zeolites 7:319-326.

[11] Corma A, Diaz-Cabanas MJ, Martinez-Triguero J, Rey F, Rius J (2002) Nature 418:514–517.

[12] Sulikowski B (1996) Heterogen Chem Rev 3:203–268.

[13] Barrer RM (1982) Hydrothermal Chemistry of Zeolites; Academic Press: London, 1982; p 251.

[14] van Bokhovena JA, Lamberti C (2014) Coord Chem Rev 277–278:275–290.

[15] Corma A, Martinez A (1995) Adv Mater 7:137-144.

[16] Ma Y, Tong W, Zhou H, Suib SL (2000) Microporous Mesoporous Mater 37:243–252.

[17] Cooper ER, Andrews CD, Wheatley PS Webb PB, Wormald P, Morris RE (2004) Nature 430:1012–1016.

[18] Vomscheid R, Briend M, Peltre MJ, Man PP, Barthoumeuf D (1994) J Phys Chem 98:9614-9618.

[19] Chen G, Sun Q, Yu QJ (2017) Chem Commun 53:13328-13331.

[20] Chen J, Natarajan S, Thomas JM, Jones RH, Hursthouse MB (1994) Angew Chem Int Ed 33:639-640.

[21] Gier ET, Stucky GD (1991) Nature 349:508–510.

[22] Wilson ST, Lok BM, Flanigen EM (1982) US Patent 4 310 440.

[23] Wilson ST, Lok BM, Messina CA, Cannan TR, Flanigen EM (1982) J Am Chem Soc 104:1146-1147.

[24] Forster PM, Eckert J, Chang JS, Park SE, Ferey G, Cheetham AK (2003) J Am Chem Soc 125:1309–1312.

[25] Parise JB (1985) J Chem Soc Chem Commun 606-607.

[26] Littlefield BTR, Weller MT (2012) Nat Commun 3:1114.

[27] Murugavel R, Choudhury A, Walawalkar MG, Pothiraja R, Rao CNR (2008) Chem Rev 108:3549–3655.

[28] Corma A, Diaz-Cabanas M, Jorda JL, Martinez C, Moliner M (2006) Nature 443:842-845.

[29] Sun J, Bonneau C, Cantin S, Corma A, Diaz-Cabanas MJ, Moliner M, Zhang D, Li M, Zou X (2009) Nature 458:1154–1157.

[30] Davis ME, Saldarriaga C, Montes C, Garces J, Crowder C (1988) Nature 331:698-699.

[31] Rouhi AM, Chem Eng News (2015) 93:30–31.

[32] Tian P, Wei YX, Ye M, Liu ZM (2015) ACS Catal 5:1922–1938.

[33] Messina CA, Lok BM, Flanigen EM (1985) US Patent 4,544,143.

[34] Wilson ST, Flanigen EM (1986) US Pat. 4,567,029.

[35] Thomas JM, Raja R, Sankar S, Bell RG (1999) Nature 398:227–230.

[36] Raja R, Sankar G, Thomas JM (1999) J Am Chem Soc 121:11926–11927.

[37] Thomas JM, Raja R, Sankar G, Bell RG (2001) Acc Chem Res 34:191–200.

[38] Ng EP, Mintova S (2008) Microporous Mesoporous Mater 114:1-26.

[39] Cheung O, Hedin N (2014) RSC Adv 4:14480-14494.

[40] Hartmann M, Kevan L (1996) J Chem Soc Faraday Trans 92:3661-3667.

[41] de Saldarriaga LS, Saldarriaga C, Davis ME (1987) J Am Chem Soc 109:2686-2691.

[42] Man PP, Briend M, Peltre MJ, Lamy A, Beaunier P, Barthomeuf D (1991) Zeolites 11, 563-572.

[43] Feng P, Bu X, Stucky GD (1997) Nature 388:735–741.

[44] Camblor MA, Corma A, Valencia S (1996) Chem Commun 2365-2366.

[45] Camblor MA, Villaescusa LA, Diaz-Cabanas MJ (1999) Top Catal 9:59-76.

[46] Lechert H (2004) Microporous Mesoporous Mater 22: 519-523.

[47] Ren X, Komarneni S, Roy DM (1991) Zeolites 11:142-148.

[48] Pourbaix M (1974) Atlas of Electrochemical Equilibria in Aqueous Solutions, NACE.

[49] Davis ME, Lobo RF (1992) Chem Mater 4:756–768.

[50] Cundy CS, Cox PA (2003) Chem Rev 103:663–702.

[51] Prasad S, Liu SB (1994) Chem Mater 6:633-635.

[52] O'Brien MG, Beale AM, Catlow CRA, Weckhuysen BM (2006) J Am Chem Soc 128: 11744-11745.

[53] Beale AM, O'Brien M, Kasunic M, Golobic A, Sanchez Sanchez M, Lobo AJW, Lewis DW, Wragg DS, Nikitenko S, Bras W, Weckhuysen BM (2011) J Phys Chem C 115:6331–6340.

[54] Valyocsik EW, Rollmann LD (1985) Zeolites 5:123-125.

[55] Ren L, Zhu L, Yang C, Chen Y, Sun Q, Zhang H, Li C, Nawaz F, Meng X, Xiao FS (2011) Chem Commun 47:9789–9791.

[56] Wilson ST, Lok BM, Messina CA, Cannan TR, Flanigen EM (1983) in Intrazeolite Chemistry (Eds. Stucky GD and Dwyer FG) ACS Symp Ser 218, Am Chem Soc, Washington, DC, p. 79.

[57] Ojo AF, McCusker LB (1991) Zeolites 11:460-465.

[58] Akolekar DB, Kaliaguine S (1993) J Chem Soc Faraday Trans 89:4141-4147.

[59] Akolekar DB (1995) Zeolites 15:583-590.

[60] Kumar R, Bhaumik A, Ahedi RK, Ganapathy S (1996) Nature 381:298-300.

[61] Annen MJ, Davis ME, Higgins JB, Schlenker JL (1991) J Chem Soc Chem Commun 1175-1176.

[62] Annen MJ, Davis ME (1993) Microporous Mater 1:57-65.

[63] Takewaki T, Beck LW, Davis ME (1999) J Phys Chem B 103, 2674-2679.

[64] Zhang X, Liu P, Wu Y, Yao Y, Wang J (2010) Catal Lett137:210–215.

[65] Flanigen EM, Lok BM, Patton RL, Wilson ST (1986) Stud Surf Sci Catal 28:103-112.

[66] Qiu S, Tian W, Pang W, Sun T, Jiang D (1991) Zeolites 11:371-375.

[67] Barthomeuf D (1994) Zeolites 14:394-401.

[68] Blasco T, Chica A, Corma A, Murphy W, Agundez-Rodriguez J, Perez-Pariente J (2006) J Catal 242:153–161.

[69] Sanchez-Sanchez M, Gomez-Hortiguela L, Sankar G (2008) Microporous Mesoporous Mater 114:485–494.

[70] Zanjanchi MA, Ghanadzadeh A, Khadem-Nahvi F (2002) J Incl Phenom Macrocycl Chem 42:295-299.

[71] Maurelli S, Vishnuvarthan M, Berlier G, Chiesa M (2012) Phys Chem Chem Phys 14:987-995.

[72] Barrett PA, Sankar G, Stephenson R, Catlow CRA, Thomas JM, Jones RH, Teat SJ (2006) Solid State Sci 8:337-341.

[73] Muncaster G, Davies AT, Sankar G, Catlow CRA, Thomas JM, Colston SL, Barnes P, Waltonc RI, O'Hare D (2000) Phys Chem Chem Phys 2:3523-3527.

[74] Sanchez-Sanchez M, Romero AA, Pinilla-Herrero I, Sastre E (2017) Catal Today 296:239–246.

[75] Duncan B, Stocker M, Gwinup D, Szotak R, Vinje V (1993) Bull Soc Chim Fr 129:98-110.

[76] McCusker LB, Baerlocher Ch, Jahn E, Bulow M (1991) Zeolites 11:308-313.

[77] Martens JA; Janssens C, Grobet PJ Beyer HK, Jacobs PA (1989) Stud Surf Sci Catal 49:215-225.

[78] Gabelica Z, Louti A, Borges C, Ribeiro MF, Lourenco, JP, Murphy, DM (2004) Stud Surf Sci Catal 154:1649-1654.

[79] Sierra L, Patarin J, Guth JL (1997) Microporous Mater 11, 19-35.

[80] Harding MM Kariuki BM (1994) Acta Cryst C50:852-854.

[81] Diaz-Cabanas MJ, Barrett PA, Camblor MA (1998) Chem Commun 1881-1882.

[82] Onyestyak G, Valyon, Rees LVC (2001) Solid State Ionics 141–142:93–97.

[83] Bejblova M, Zones SI, Cejka J (2007) Appl Catal A Gen 327:255–260.

[84] Sanchez-Sanchez M, Sankar G, Simperler A, Bell RG, Catlow CRA, Thomas JM (2003) Catal Lett 88:163-168.

[85] Davies AT, Sankar G, Catlow CRA, Clark SM (1997) J Phys Chem 101:10115-10120.

[86] Zenonos C, Sankar G, Cora F, Lewis DW, Pankhurst AQ, Catlow CRA, Thomas JM (2002) Phys Chem Chem Phys 4, 5421-5429.

[87] Patinec V, Wright PA, Lightfoot P, Aitken RA, Cox PA (1999) J Chem Soc Dalton Trans 3909-3911.

[88] Garcia R, Philp EP, Slawin AMZ, Wright PA, Cox PA (2001) J Mater Chem 11:1421-1427.

[89] Grosse-Kunstleve RW, McCusker LB, Baerlocher Ch (1997) J Appl Cryst 30:985-995.

[90] Inge AK, Fahlquist H, Willhammar T, Huang Y, McCusker LB, Zou X (2013) J Appl Cryst 46:1094-1104.

[91] McCusker LB (1991) Acta Cryst A47:297-313.

[92] McCusker LB (1994) Stud Surf Sci Catal 84:341-356.

[93] Wright PA (2008) ‘Microporous Framework Solids’ RSC Materials Monographs 79-147.

[94] Gramm F, Baerlocher Ch, McCusker LB, Warrender SJ, Wright PA, Han B, Hong SB, Liu Z, Ohsuna T, Terasaki O (2006) Nature 444:79–81.

[95] Sun J, He Z, Hovmoller S, Zou X, Gramm F, Baerlocher Ch, McCusker LB (2010) z Kristallogr Cryst. Mater 225:77–85.

[96] Wright PA, Natarajan S, Thomas JM, Bell RG, Gai-Boyes PL, Jones RH, Chen J (1992) Angew Chem Int Ed 31:1472-1475.

[97] Barrett PA, Jones RH (2000) Phys Chem Chem Phys 2:407–412.

[98] Sankar G, Wyles JK, Jones RH, Thomas JM, Catlow CRA, Lewis DW, Clegg W, Coles SJ, Teat SJ (1998) Chem Commun 117-118.

[99] Simmance K, Sankar G, Bell RG, Prestipino C, van Beek W (2010) Phys Chem Chem Phys 12:559–562.

[100] Simmance K, van Beek W, Sankar G (2015) Faraday Discuss 177:237-247.

[101] Canesson L, Tuel A (1997) Chem Commun 241:242.

[102] Canesson L, Boudeville Y, Tuel A (1997) J Am Chem Soc 119:10754-10762.

[103] Barrie PJ, Klinowski j (1989) J. Phys. Chem., 93:5972-5974.

[104] Shea WL, Borade RB, Clearfield A, (1993) J Chem Soc Faraday Trans 89 3143:3149.

[105] Tuel A, Arcon I, Tusar NN, Meden A, Kaucic V (1996) Microporous Mater 7:271-284.

[106] Alfayate A, Sanchez-Sanchez M, Perez-Pariente J (2014) Microporous Mesoporous Mater 190:334-345.

[107] Schoonheydt RA, De Vos R, Pelgrims J, Leeman H (1989) Stud Surf Sci Catal 49: 559-568.

[108] Kraushaar-Czarnetzki B, Hoogervorst WGM, Andrea RR, Emeis CA, Stork WHJ (1991) J Chem Soc Faraday Trans 87:891-895.

[109] Uytterhoeven MG, Schoonheydt RA (1994) Microporous Mater 3:265-279.

[110] Nakashiro K, Ono Y (1993) Bull Chem Soc Jpn 66:9-17.

[111] Verberckmoes AA, Uytterhoeven MG, Schoonheydt RA (1997) Zeolites 19:180-189.

[112] Verberckmoes AA, Uytterhoeven MG, Schoonheydt RA (1998) Microporous Mesoporous Mater 22:165-178.

[113] Weckhuysen BM, Rao RR, Martens JA, Schoonheydt RA (1999) Eur J Inorg Chem 565-577.

[114] Tusar NN, Mali G, Arcon I, Kaucic V, Ghanbari-Siahkali A, Dwyer J (2002) Microporous and Mesoporous Mater 55:203–216.

[115] Weckhuysen BM, Verberckmoes AA, Uytterhoeven MG, Mabbs FE, Collison D, de Boer E, Schoonheydt RA (2000) J Phys Chem B 104:37-42.

[116] Barrett PA, Sankar G, Catlow CRA, Thomas JM (1996) J Phys Chem 100:8977-8985.

[117] Chen J, Thomas JM (1994) J Chem Soc Chem Commun 603-604.

[118] Chen J, Thomas JM, Sankar G (1994) J Chem Soc Faraday Trans 90:3455-3459

[119] Thomas JM, Greaves GN, Sankar G, Wright PA, Chen J, Dent AJ, Marchese L (1994) Angew Chem Int Ed 33:1871–1873.

[120] Hartmann M, Elangovan SP (2009) Adv Nanoporous Mater 1: 237-312.

[121] Hartmann M, Kevan L (1999) Chem Rev 99:635-663.

[122] Hartmann M, Kevan L (2002) Res Chem Intermed 28:625-695.

[123] Kurshev V, Kevan L, Parillo DJ, Pereira C, Kokotailo GT, Gorte RJ (1994) J Phys Chem 98:10160-10166.

[124] Nagarajan V, Rings D, Moschkowitz L, Hartmann M, Poppl A (2005) Chem Lett 34:1614-1615.

[125] Prakash AM, Hartmann M, Zhu Z, Kevan L (2000) J Phys Chem B 104:1610-1616.

[126] Prakash AM, Kevan L (1999) J Phys Chem 103:2214-2222.

[127] Zahedi-Niaki MH, Kaliaguine S (1999) J Phys Chem B 103:831-837.

[128] Prakash AM, Kurshev V, Kevan L (1997) J Phys Chem B 101:9794-9799.

[129] Zhu Z, Kevan L (1999) Phys Chem Chem Phys 1:199-206.

[130] Beale AM, Sankar G, Catlow CRA, Anderson PA, Green TL (2005) Phys Chem Chem Phys 7:1856-1860.

[131] Cora F, Sankar G, Catlow CRA, Thomas JM (2002) Chem Commun 734-735.

[132] Franklin IL, Beale AM, Sankar G (2003) Catal Today 81:623-629.

[133] Ono Y (2003) J Catal 216:406-415.

[134] Zhang HX, Chokkalingam A, Subramaniam PV, Joseph S, Takeuchi S, Wei MD, Al-Enizi AM, Jang HG, Kim JH, Seo G, Komura K, Sugi Y, Vinu A (2016) J Mol Catal A Chem 412:117-124.

[135] Concepcion P, Lopez Nieto JM, Mifsud A, Perez-Pariente J (1997) Appl Catal A Gen 151:373-392.

[136] Fan W, Fan B, Song M, Chen T, Li R, Dou T, Tatsumi T, Weckhuysen BM (2006) Microporous Mesoporous Mater 94:348-357.

[137] Masters AF, Beattie JK, Roa AL (2001) Catal Lett 75:159-162.

[138] Moden B, Zhan BZ, Dakka J, Santiesteban JG, Iglesia E (2007) J Phys Chem C 111:1402-1411.

[139] Schuchardt U, Cardoso D, Sercheli R, Pereira R, da Cruz RS, Guerreiro MC, Mandelli D, Spinace EV, Pires EL (2001) Appl Catal A Gen 211:1-17.

[140] Vanoppen DL, De Vos DE, Genet MJ, Rouxhet PG, Jacobs PA Angew Chem Int Ed 34:560-563.

[141] Wang XH, Li J, Wan YJ, Yan JL, Zhang BQ, LiuXF (2010) Chin Sci Bull 55:4112-4115.

[142] Moden B, Oliviero L, Dakka J, Santiesteban JG, Iglesia E (2004) J Phys Chem B 108:5552-5563.

[143] Moden B, Zhan BZ, Dakka J, Santiesteban JG, Iglesia E (2006) J Catal 239:390-401.

[144] Dugal M, Sankar G, Raja R, Thomas JM (2000) Angew Chem Int Ed 39:2310-2313.

[145] Sankar G, Raja R, Thomas JM (1998) Catal Lett 55:15-23.

[146] Raja R, Sankar G, Thomas JM (2000) Angew Chem Int Ed 39:2313-2316.

[147] Cora F, Gomez-Hortiguela L, Catlow CRA (2012) Proc R Soc A 468:2053-2069.

[148] Gomez-Hortiguela L, Cora F, Catlow CRA (2011) ACS Catal 1:18-28

[149] Gomez-Hortiguela L, Cora F, Catlow CRA (2011) ACS Catal 1:945-955.

[150] Gomez-Hortiguela L, Cora F, Catlow CRA (2011) ACS Catal 1:1487-1497.

[151] Gomez-Hortiguela L, Cora F, Catlow CRA (2011) ACS Catal 1:1475-1486.

[152] Gomez-Hortiguela L, Cora F, Catlow CRA (2012) J Phys Chem C 116:6691-6702.

[153] Gomez-Hortiguela L, Cora F, Catlow CRA (2013) Phys Chem Chem Phys 15:6870-6874.

[154] Gomez-Hortiguela L, Cora F, Sankar G, Zicovich-Wilson C, Catlow CRA (2010) Chem Eur J 16:13638-13645.

[155] Gomez-Hortiguela L, Cora F, Catlow CRA (2013) Modelling and Simulation in the Science of Micro- and Meso-Porous Materials, Ed. Elsevier, 265-295.

[156] Raja R, Lee SO, Sanchez-Sanchez M, Sankar G, Harris KDM, Johnson BFG, Thomas JM (2002) Top Catal 20:85-88.

[157] Potter ME, Paterson AJ, Raja R (2012) ACS Catal 2:2446-2451.

[158] Shiju NR, Fiddy S, Sonntag O, Stockenhuber M, Sankar G (2006) Chem Commun 4955-4957.

[159] Wei W, Moulijn JA, Mul G (2008) Microporous Mesoporous Mater 112:193-201.

[160] Raja R, Thomas JM, Sankar G (1999) Chem Commun 829-830

[161] Raja R, Thomas JM, Sankar G (1999) Chem Commun 525-526.

[162] Hentit H, Bachari K, Ouali MS, Womes M, Benaichouba B, Jumas JC (2007) J Mol Catal A Chem 275:158–166.

[163] Raja R, Sankar G, Thomas JM (2001) J Am Chem Soc 123:8153-8154.

[164] Chatterjee S, Bhanja P, Paul L, Bhaumik A, Dalton Trans (2018) 47:791-798.

[165] Wu JY, Chien SH, Wan BZ (2001) Ind Eng Chem Res 40:94-100.

[166] Zahedi-Niaki MH, Xu GY, Meyer H, Fyfe CA, Kaliaguine S (1999) Microporous Mesoporous Mater. 32:241-250.

[167] Li J, Yu J, Xu R (2012) Proc R Soc A 468:1955–1967.

[168] Sanchez-Sanchez M, Serrano DP, van Grieken R, Melero JA (2007) Stud Surf Sci Catal 170:499-505.

[169] Wright PA, Jones RH, Natarajan S, Bell RG, Chen JS, Hursthouse MB, Thomas JM (1993) J Chem Soc Chem Commun 633-635.

[170] Yu J, Xu R, (2010) Acc Chem Res 43:1195–1204.

[171] Sanchez-Sanchez M, Sankar G (2004) Stud Surf Sci Catal 154:1021-1027.

[172] Lok BM, Cannan TR, Messina CA (1983) Zeolites 3:282-291.

[173] Cundy CS, Cox PA (2005) Microporous Mesoporous Mater 82, 1-78.

[174] Alvaro-Munoz T, Marquez-Alvarez C, Sastre E (2012) Catal Today 179:27-34.

[175] Akolekar DB (1993) J Catal 143:227-238.

[176] Flanigen EM, Lok BM, Patton RL, Wilson ST (1986) Pure Appl Chem 58:1351-1358.

[177] Nakashiro K, Ono Y (1991) J Chem Soc Faraday Trans 87:3309-3313.

[178] Machado MS, Perez-Pariente J, Sastre E, Cardoso D, Giotto MV, Garcia-Fierro JL, Fornes V (2002) J Catal 205:299–308.

[179] Akolekar DB (1994) Catal Lett 28:249–262.

[180] Manjon-Sanz A, Sanchez-Sanchez M, Munoz-Gomez P, Garcia R, Sastre E (2010) Microporous Mesoporous Mater 131:331-341.

[181] Manjon-Sanz A, Sanchez-Sanchez M, Sastre E (2012) Catal Today 179:102-114.

[182] Roldan R, Sanchez-Sanchez M, Sankar G, Romero-Salguero FJ, Jimenez-Sanchidrian C (2007) Microporous Mesoporous Mater 99:288-298.

[183] Jhung SH, Hwang YK, Chang JS, Park SE (2004) Microporous Mesoporous Mater 67:151-157.

[184] Egeblad K, Christensen CH, Kustova M, Christensen CH (2008) Chem Mater 20, 946-960.

[185] Karanikolos GN, Garcia H, Corma A, Tsapatsis M (2008) Microporous Mesoporous Mater 115, 11-22.

[186] Veziri CM, Palomino M, Karanikolos GN, Corma A, Kanellopoulos NK, Tsapatsis M (2010) Chem Mater 22:1492-1502.

[187] Wu LL, Hensen EJM (2014) Catal Today 235:160-168.

[188] Bonilla MR, Valiullin R, Karger J, Bhatia SK (2014) J Phys Chem C 118:14355-14370.

[189] Schmidt I, Madsen C, Jacobsen CJH (2000) Inorg Chem 2000, 39, 2279-2283.

[190] Jacobsen CJH, Madsen C, Houzvicka J, Schmidt I, Carlsson A (2000) J Am Chem Soc 122:7116-7117.

[191] Sanchez-Sanchez M, Manjon-Sanz A, Diaz I, Mayoral A, Sastre S (2013) Cryst Growth Des 13:2476-2485.

[192] Renz M, Blasco T, Corma A, Fornes V, Jensen R, Nemeth L (2002) Chem Eur J 8:4708-4716.

[193] Corma A, Domine ME, Nemeth L, Valencia S (2002) J Am Chem Soc 124:3194-3195.

[194] Sanchez-Sanchez M, van Grieken R, Serrano DP, Melero JA (2009) J Mater Chem 19:6833–6841.

[195] Taramasso M, Perego G, Notari B (1983) US Patent 4,410,501.

[196] Notari B (1996) Adv Catal 41:253-334.

[197] Corma A, Camblor MA, Esteve P, Martinez A, Perez-Pariente J (1994) J Catal 145:151-158.

[198] Torres JC, Cardoso, Pereira R (2010) Microporous Mesoporous Mater 136:97-105.

[199] Alfayate A, Marquez-Alvarez C, Grande-Casas M, Bernardo-Maestro B, Sanchez-Sanchez M, Perez-Pariente J (2013) Catal Today 213:211- 218.

[200] Alfayate A, Marquez-Alvarez C, Grande-Casas M, Sanchez-Sanchez M, Perez-Pariente J (2014) Catal Today 227:57–64.

[201] Mayoral A, Sanchez-Sanchez M, Alfayate M, Perez-Pariente J, Diaz I (2015) ChemCatChem 7:3719 – 3724

[202] Alfayate A, Sepulveda R, Sanchez-Sanchez M, Perez-Pariente J (2016) Top Catal 59:326–336.

[203] Ovejero G, van Grieken R, Uguina MA, Serrano DP, Melero, JA (1996) Catal Lett 41: 69-78.

[204] Winoto HP, Ahn BS, Jae JJ (2016) Ind Eng Chem 40:62-71.

[205] Padovan D, Al-Nayili A, Hammond C (2017) Green Chem 19:2846-2854.

[206] Tuel A, Taarit YB (1994) J Chem Soc Chem Commun 14:1667-1668.

[207] Blasco T, Fernandez L, Martinez-Arias A, Sanchez-Sanchez M, Concepcion P, Lopez-Nieto JM (2000) Microporous Mesoporous Mater 39:219-228.

[208] Gianotti E, Manzoli M, Potter ME, Shetti VN, Sun D, Paterson J, Mezza TM, Levy A, Raja R (2014) Chem Sci 5:1810-1819.

[209] Zhou LP, Xu J, Chen C, Wang F, Li XQ (2008) J Porous Mater 15:7-12.

[210] Potter ME, Paterson AJ, Raja R (2012) ACS Catal 2:2446-2451.

[211] Leithall RM, Shetti VN, Maurelli S, Chiesa M, Gianotti E, Raja R (2013) J Am Chem Soc 135:2915-2918.

[212] O’Brien MG, Sanchez-Sanchez M, Beale AM, Lewis DW, Sankar G, Catlow CRA (2007) J Phys Chem C 111:16951-16961.

[213] Harris TV, Zones SI (1994) Stud Surf Sci Catal 84:29-36.